

POLITECNICO DI TORINO

**MASTER OF SCIENCE IN MECHATRONIC
ENGINEERING**



Master's Degree Thesis

**Controlling car braking by means of
electromechanical actuation on the pedal**

Supervisors

Prof. CARLO NOVARA

Co-Sup. CLAUDIO RUSSO

Candidate

RAFFAELE VALENTINI

DECEMBER 2021

Summary

This thesis work aims to implement an autonomous braking system on a pre-assembled car and has been developed with the company Bylogix s.r.l.

The main goal of this thesis is to design an Advanced Driver Assistance System (ADAS) implementable on a real vehicle, with the relative control system able to follow the target speed required by the autonomous driving system. An electromechanical actuator has been designed to operate as the interface between the autonomous driving and the brake pedal.

The state-of-art systems are Brake-By-Wire solutions, which require a radical modification of the vehicle. The technology proposed in this dissertation is less invasive and more redundant than the BBW.

The braking manoeuvre has been studied empirically and analytically, in order to have the proper basis for the design choices. The plant composed by the typical hydraulic braking system has been modelled using studies and methods already present in literature.

The control actuation goals has been defined and designed in order to fulfill all the mechanical requirements. The model generated is useful to evaluate the physical quantities which interact within the whole system, in order to design a control system enough robust to operate in any braking condition.

Considering that the treated system is Nonlinear, the control approach was opted for a Hybrid Gain Scheduling. The operating points have been analyzed and divided in two regions in which it is possible to use a linear PID controller for each one.

The first controller is used for normal braking, which lowers the speed down to the input target speed selected by the autonomous driving pilot with possibly the smoothest deceleration.

The second controller is used for emergency braking, occurring in exceptionally alarming situations, when a hard braking is required to prevent harmful conditions. In this case the input is the optimal slip of the wheel to obtain the best deceleration without losing the drivability.

The interpolation between the two controllers is entrusted to a proper designed switch logic, which is composed by a comparator with hysteresis and the optimal slip value as reference.

The system model has been implemented on Simulink and tested using different road tyre condition and with the addition of time delays and uncertainties on the grip coefficient, in order to simulate real driving scenarios.

In conclusion the system can be consider robust and suitable to follow the target speed required from the autonomous driving system. In particular it can provide a smooth and comfortable braking in normal scenarios and a safe and fast deceleration in case of urgency braking.

Acknowledgements

“The cosmos is within us. We are made of star-stuff. We are a way for the universe to know itself”
Cosmos - Carl Sagan

Questa Tesi è l'ultimo significativo passo della mia carriera universitaria, che mi ha reso quello che sono ora come studente, lavoratore ma soprattutto come persona. Come, credo, in tutti i traguardi umani, quando si arriva alla metaforica "bandiera a scacchi" c'è sempre un dietro le quinte, fatto di numerose difficoltà e gioie, che solamente un'esperienza così significativa come un percorso universitario ti può lasciare. Nel dietro le quinte ci sono soprattutto tutte le persone che mi hanno permesso di arrivare a questo traguardo, a cui devo molto.

Vorrei ringraziare il Professore Carlo Novara per l'opportunità ed il supporto nella stesura di un argomento di Tesi che rispecchia in pieno i miei interessi. Un ringraziamento a tutta l'azienda Bylogix, per avermi accolto e supportato nel migliore dei modi ed al mio tutor Claudio Russo che mi ha guidato e consigliato quando ce n'è stato bisogno e non solo sugli argomenti della Tesi.

Grazie alla mia famiglia, a mia Mamma che non ha mai perso l'occasione di ricordarmi quanto valgo e quanto nella vita occorra mettersi in gioco per raggiungere i propri obiettivi, a mio Padre che mi ha trasmesso le passioni che mi hanno reso quello che sono e per il modello di persona che vorrei essere soprattutto nell'affrontare i problemi della vita, a mia sorella per la spensieratezza che mi ha sempre donato con la sua presenza e per gli infiniti consigli. Ai miei nonni/e Antonia, Liliana, Lorenzo e Salvatore per tutto l'amore e per gli insegnamenti che porterò sempre, gelosamente, con me.

Un grazie ai miei amici di sempre con cui sono cresciuto, per tutti i ricordi indimenticabili che mi avete regalato e per farmi sentire di nuovo a casa ogni volta che torno. Ai miei coinquilini del Chicco d'oro, vecchio e nuovo, la mia seconda

casa, i miei fratelli acquisiti, grazie. Ringrazio anche tutti i miei amici "Torinesi" e le persone che mi hanno accompagnato e sostenuto in questi anni. Senza il supporto di tutte queste persone, sono certo che il mio percorso universitario sarebbe stato più difficoltoso e vuoto.

Table of Contents

1	Introduction	1
1.1	Thesis structure	3
2	Car braking background	4
2.1	Definition and regulations	4
2.1.1	Complex electronic vehicle system	7
2.2	Braking sequence	8
2.2.1	Stopping the vehicle	10
2.2.2	Decelerating by braking	10
3	Vehicle dynamics	12
3.1	Longitudinal dynamics	12
3.1.1	Grip coefficient and Slip Ratio	14
3.1.2	Burckhardt model	16
3.2	Lateral Dynamics	18
3.2.1	Kamm circle	20
4	Model of braking system	21
4.1	Single-Wheel Model	21
4.2	Disc Brake	24
4.3	Brake Hydraulic System	27
4.3.1	Master Cylinder	27
4.3.2	Brake circuit	29
4.3.3	Brake booster	29
4.3.4	Brake vacuum booster + TMC	29
4.3.5	Pedal	31
4.4	Whole Braking System	33
5	Design of Braking Actuator System	34
5.1	Design contest	34
5.2	Mechanical Model	35

5.3	Servo DC motor	37
6	Control system design	39
6.1	Block diagrams	39
6.2	Model Analysis	42
6.2.1	Equilibrium points	42
6.2.2	Model Linearization and Stability Analysis	43
6.3	Control approach	46
6.4	Switch Logic	47
6.5	Optimal slip	49
7	Simulations results	52
7.1	Hard braking test	54
7.1.1	Without slip PID controller	54
7.1.2	Using slip PID controller	56
7.1.3	Different road conditions: Wet asphalt	58
7.1.4	Different road conditions: Snow	62
7.2	Drive Cycle test	67
8	Conclusions	69
8.1	Future works	70
A	Gain scheduling	71

Chapter 1

Introduction

The autonomous driving paradigm started to propel the automotive field, this new feature needs to automate steering, acceleration and deceleration, the fundamental actions used to drive a car.

This thesis focuses on the development of an autonomous braking control that must be stable and suitable in the real world.

The system designed must reach the safety and performance standard, in order to avoid harm to the individuals and things involved during a car braking.

The most used braking solution in self-driving cars is the brake-by-wire system (BBW) which controls braking and other basic car functions through electrical actuators.

The state-of-art BBW systems are the electro-hydraulic brake (EHB) and electro-mechanical brake (EMB) which have good response speed and flexibility, but are made from expensive and not readily available components and require deep changes in the vehicle structure in order to function [1],[2].

More time is required to design and tune the BBW compared to the classical hydraulic braking system.

It is cumbersome to reach a good compromise between performance and costs with this approach, indeed until now it is missing a technical consensus about BBW from the automotive sector [3].

Cars are commonly provided with the Anti-lock Braking System (ABS) which uses electrical-valves to decrease the pressure in the brake's hydraulic circuit. This sudden decrease of pressure keeps the car in the stable area of braking maneuver [4].

Reference [5] explains how the ABS control may improve braking performance with a direct maximization of the tyre-road grip coefficient, especially under critical friction condition.

Together with Bylogix s.r.l. we developed a solution to actuate the legacy, pre-installed braking system of a car directly operating on its braking pedal with an electric DC motor and leveraging a specifically designed mechanical system. This solution is purposely designed for the experimental autonomous vehicle which the company is developing.

This designed system can be considered an interface between the autonomous driving system and the hydraulic braking system already present on common vehicles. In opposite to the BBW, the presented solution allows to maintain the reliability achieved in the recent decade by the conventional braking system.

The system designed can be implemented with components and actuators already used in many applications, so that it is possible to have a wide choice in terms of price and performance.

The system always provides the brake control to the driver, even in case of system failure, due to the fact that the pedal is still directly connected with the braking system.

In this project the control system used for the autonomous braking is the Hybrid Gain Scheduling. It allows the use of LTI control design as the PID controller also in the nonlinear system treated in this thesis.

Two different controllers have been developed for each of the two operational regions of the system:

1. PID - Speed error control is used for the normal braking regime. The gain values of the PID controller are tuned to reach the speed target rapidly and smoothly enough as to avoid loss of comfort. In this region the control input is the speed error and the slip ratio is in the stable region;
2. PID - Slip ratio control is used for emergency braking, when the slip ratio is near to the critical value. The gain values of the PID controller are tuned to reach the slip ratio target as fast as possible in order to return in the stable slip interval and avoiding loss of control of the car. The control input is the slip ratio error and the slip ratio is in the unstable region;

A proper switch logic has been designed in order to manage the switching between the two PIDs. The value used as reference is the optimal slip ratio, estimated in real-time using a method developed in this Thesis. The optimal slip ratio is evaluated using the derivative of the grip coefficient.

Considering the aforementioned reasons, the solution proposed in this thesis is appealing for a short term implementation in the autonomous driving field. In a long term perspective, this technology represents a promising research field and could also replace the BBW system in an industrial context with the proper integration for the particular use case and improvements.

1.1 Thesis structure

The regulations, the definition and the different typologies of car braking are presented in the following chapter. This empirical study is useful as an introduction to the related context and to give a solid basis for the problem analysis.

In the third chapter, it is treated the longitudinal and the lateral dynamics for the vehicle braking, giving a mathematical formulation of the problem and presenting the parameters and the physical quantities involved.

The following chapter is focused on the analysis and subsequent generation of the plant model. The braking system has been divided in components, in order to ease the modelling.

Then, in the fifth chapter the electromechanical actuator used as interface between brake pedal and autonomous driving system is explained, designed and modelled.

The sixth chapter is focused on the model stability analysis and control system design. The developed Hybrid Gain scheduling and the switch logic are introduced and the relative design choices are explained.

Finally, the whole braking autonomous system model is simulated using the software Simulink provided by Matlab. The test used allows to evaluate and validate the performance of the system within different configurations.

In the last chapter, the results are analyzed in the conclusions, giving at detailed overview of this thesis work and giving some suggestions for future research works.

Chapter 2

Car braking background

2.1 Definition and regulations

The braking system is defined by the European Union regulations [6] as the combination of components whose intent is to reduce the speed of a vehicle, bring it to a stop state or to keep it stationary if it is already in a stop state.

This study is focused on the classical service braking system that consists in disk brakes with a hydraulic transmission and brake control, available to the driver by means of the pedal in the driver footrest.

The vehicle used is the **Citroën e-Méhari**: a full-electric cabriolet, included in the M1 vehicle category. The United Nations Economic Commission for Europe [7] defines this category as motor vehicles having at least four wheels and used for the carriage of passengers, comprising not more than eight seats in addition to the driver's.

The braking system must be composed by three main parts:

1. The **brake** is the device developing forces opposed to vehicle motion. The main types used in the automotive applications are:
 - Friction brakes: when the brakes forces are developed by friction between two parts of the vehicle (e.g. Drum and Disk brakes);
 - Electric brakes: when braking forces are developed by an electro-magnetic action between parts with relative motion, but not in contact (e.g. DC motor brush-less);
 - Engine brake: when the braking forces are produced by an artificial increase of the engine braking effect;
2. The **control** consists in devices/parts that are used to provide the energy required to brake or to control the brakes. The control is directly operated by

the driver or, eventually, by an autonomous system. The simplest example is the brake pedal.

3. The **transmission** is defined by the Directive as the combination of devices that allows the connection between the control and the brake. It can be mechanical, hydraulic, pneumatic, electric or mixed (e.g. the hydraulic brake system used in the common vehicle).

The transmission has two independent functions:

- Control transmission: the parts of transmission which have the task to carry the signals/information about the operation of the brakes.
- Energy transmission: the parts of transmission which have the task to supply to the brakes the necessary energy for their function.

A complete braking system must be able to provide these functionalities to the user [8]:

- ✓ Stop the vehicle as soon as possible in the shortest possible distance;
- ✓ Modulate in a smooth and controllable way the vehicle speed, in any driving situation;
- ✓ Maintain the vehicle in stationary position in any slope condition, even if the driver is not present;

In case of failure of critical components, the functionalities listed above are expected to provide a minimum performance level. In order to reach them the European regulations requires three braking system:

1. The **Service braking system** must allow vehicle speed control, stopping it quickly and safely at any speed or load conditions. The driver or the autonomous system shall be able to tune the braking action;
2. The **Secondary braking system** must allow to stop the vehicle in a reasonable space, when the service brake is malfunctioning. It should be possible to tune this braking function;
3. The **Parking braking system** must allow the vehicle to remain still in any road and slope conditions, even if the user is not present;

These systems can have common devices/components. For example, the Secondary and Parking braking system should be included both in a classical hand brake.

In addition, they must satisfy the following requirements:

- There are at least two independent control devices;

- The control service braking system shall be independent from the parking brake control;
- Each control must return to the rest position when released (there is an exception for the parking brake system);
- If there are a separate control for the service braking system and the secondary braking system, both systems must continue to work also when one of them is faulty and also when both are used at the same time;

There are limits on the minimum and maximum force to be applied on the brake pedal to pass the braking tests, indeed it is required to verify that is possible to obtain all deceleration levels prescribed for any maneuver required to the vehicle. The pedal limit effort must be between 6.5 and 50 daN where the unit of measure $1 \text{ daN} = 10 \text{ N} \approx 1 \text{ kg} \cdot 9.81 \text{ m/s}^2$.

Typically, in the vehicle it is installed a device called “servo” or “booster” able to provide power assistance to the driver in order to reduce the effort required to use the control of braking system.

The ideal conditions for the braking system are reached if there are cold brakes, met when the temperature measured on the disks is less than 100°C , and a high friction coefficient between tire and road, corresponding to a value greater than 0.5 for dry road. In order to have a complete perspective of the braking action, also the not ideal condition must be analyzed that occurs when brakes temperature is $>100^\circ\text{C}$ or when friction coefficient is <0.5 .

When the braking systems are developed it is necessary to consider the dynamics of brakes force at each axle and wheel in terms of brake force distribution due to the longitudinal and lateral weight transfer and condition parameters such as friction coefficient and vehicle braking efficiency.

In the braking maneuver, also the golden rules for the Eco-drive must be taken into account:

- Maintain a steady state speed. Use the highest gear possible and drive with low engine rpm. The engine will work in a more efficient part of the FC map;
- Anticipate traffic flow. Look ahead as far as possible and anticipate to surrounding traffic;
- Decelerate smoothly by releasing the accelerator in time, leaving the vehicle in gear;

2.1.1 Complex electronic vehicle system

In the last years, the field research has focused on the need to provide an intelligent control used to improve the safety of the braking maneuver, through the utilization of complex electronic vehicle control system such as antilock braking (ABS), Electronic Brake Distribution (EBD), Electronic, Stability Control (ESC) and autonomous braking.

The complex electronic vehicle system is controlled by software and is built from discrete functional components such as sensors, electronic control units (ECU) and actuators, which are all connected by transmission link and can include mechanical, electro-mechanical, electro-pneumatic or electro-hydraulic elements. This system can over-ride other system in the vehicle to reach its objectives, using a well-defined hierarchy with priorities.

In the phase of design of complex electronic vehicle systems, it is mandatory to use the international standard **ISO-26262** [9], to have the reliability and the robustness necessary for this sensitive topic. The system must be evaluated in terms of ASIL level, which is useful to find the methods and measures that are necessary to achieve the safety goals.

The safety goals describe all the functionalities that the item must provide in order to avoid the hazard. The functional safety concept regard all the accessory service implemented on the system in order to guarantee the correct achievements of the safety goals.

The safe state is a state of the system in which, even if the item is not working at all or not working properly, the user takes no risk deriving from this malfunction. Furthermore, if it occurs these conditions of the system, the user must be informed properly.

In general, when there is a failure of the electronic system, one of its components (e.g. power supply or wiring), the control system or a sensor, the failure must be signaled to the driver and, possibly, to the autonomous system.

The system designed in this thesis work, with respect to a classical brake-by-wire system, has a mechanical safety redundancy. The human driver can always control the braking system, so that if the autonomous braking system is in failure, the user can stop the vehicle.

2.2 Braking sequence

The vehicle braking sequence has to keep into account the vehicle deceleration, speed, distance, brake-line pressure and the actuating device travel (e.g. pedal travel).[10]

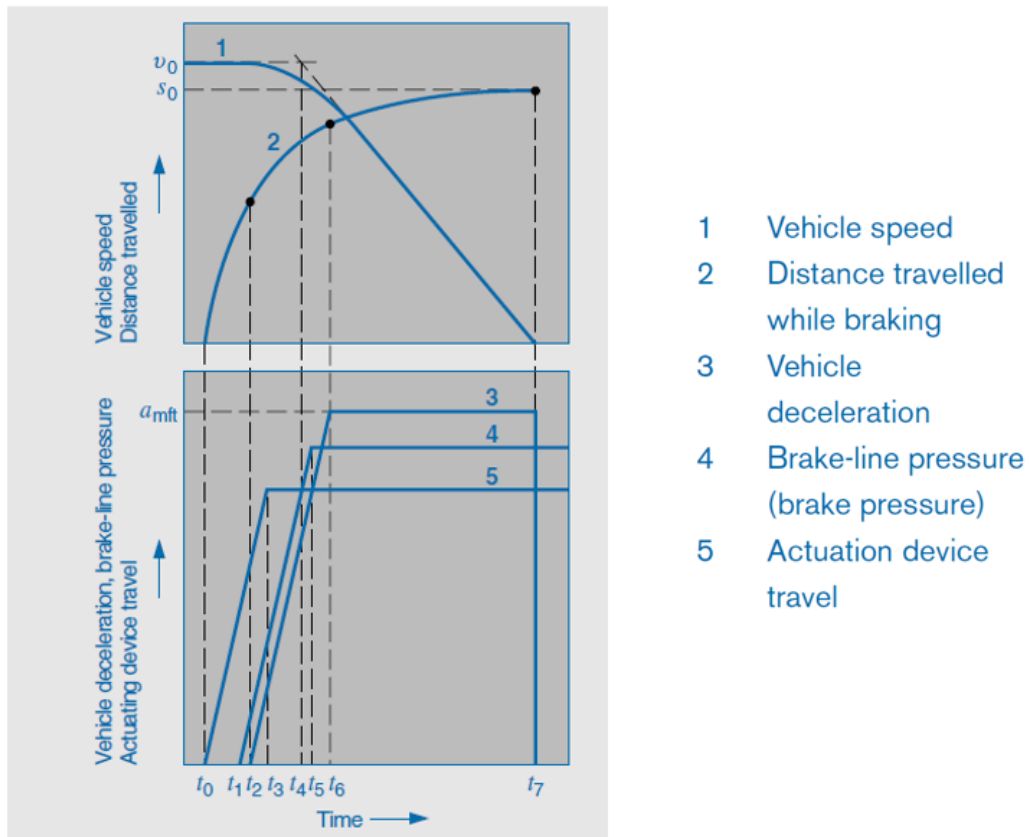


Figure 2.1: Vehicle braking sequence [10]

With reference to Figure (2.1), the points in time are:

t_0 : Time at which the driver first applies force to actuation device;

t_1 : Brake-line pressure starts to rise;

t_2 : Vehicle deceleration begins;

t_3 : Actuation device has reached intended position;

t_4 : Intersection of extended speed curve sections;

t_5 : Brake-line pressure has reached stabilized level;

t_6 : Vehicle deceleration has reached stabilized level;

t_7 : Braking force ceases or the vehicle comes to a halt;

Using the time points explained above it is possible to define these intervals:

- Period of movement of actuation device ($t_3 - t_0$): it is the time from t_0 to the moment when it reaches its final position t_3 , as determined by the actuating force. The same applies by analogy to the release of the brakes;
- Response time ($t_a = t_1 - t_0$): it is the time from t_0 to the moment when braking force is first applied;
- Total braking time ($t_b = t_7 - t_0$): it is the time from t_0 to the moment when the braking force ceases;
- Pressure build up time ($t_s = t_5 - t_1$): it is the time from t_1 to the moment when the pressure in brakes line reaches its highest level;
- Effective braking time ($t_w = t_7 - t_2$): it is the time that elapses from the moment when the braking force is first produced t_2 , to the moment when the braking force ceases t_7 ;

Referring to Figure (2.1), we can also define:

- Total braking distance s_0 is the distance travelled by a vehicle during the period of the total braking time ($t_7 - t_0$);
- Initial vehicle speed v_0 at time t_0 ;
- Mean fully developed deceleration a_m is the quotient of the reduction in speed and brakes time interval $a_m = \Delta V / \Delta t$, where $\Delta V = V_f - V_i$. This value can be used as a target value to modulate the decreasing of the speed;

These elements are collected during tests and simulations to evaluate the performance of the vehicle braking system.

The decelerating by braking could be seen in Figure (2.2) as a control closed loop between the driver and the vehicle.

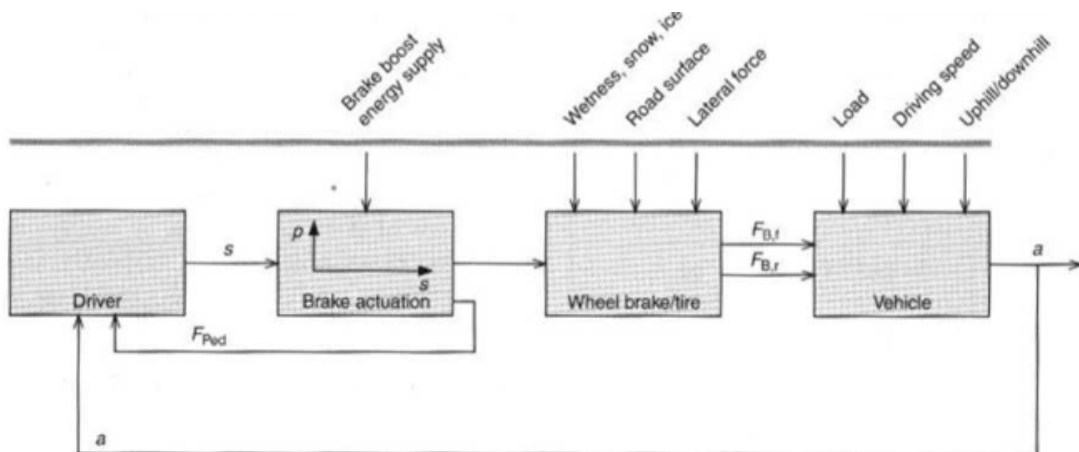


Figure 2.2: Braking closed-loop [11]

This feedback loop can be modified using an autonomous system replacing the driver block.

2.2.1 Stopping the vehicle

The vehicle is stopped when it switches from a motion to a static status. The braking system is used to stop the vehicle in the following situations:

1. The vehicle must be stopped to park or respect the road laws (e.g. the stop signal);
2. To stop the vehicle in presence of an obstacle on the vehicle way (e.g. unexpected pedestrian road cross);
3. In occurrence of a critical situation (e.g. engine stop working) when there is the necessity to bring the vehicle in a safe state;

2.2.2 Decelerating by braking

The aim of a deceleration is to change the velocity in a safe and smooth way, in order to have the best possible comfort for the users, avoid an excessive use of the brakes and reduce brake wear as much as possible.

The braking system is used for decelerating the vehicle when it is necessary to:

- Maintain a safe distance from the preceding vehicle;
- Reduce the speed in order to not exceed the speed limit of the road;
- Reduce the speed in order to take a bend or avoid an obstacle;

- Modulate the speed in the case of a road with slope not equal to 0° ;

In normal driving conditions, the vehicle deceleration rate rarely exceeds the benchmark value of $3.4 m/s^2$ proposed as the limit comfortable deceleration rate by AASHTO (American Association of State Highway and Transportation Officials) [12].

Chapter 3

Vehicle dynamics

A car is a complex system consisting of many elements, each one influencing the dynamics of the vehicle, that must be described with a large number of variables and physical quantities.

The following chapter is focused on the definition of the braking manoeuvre analyzing two different perspectives: the longitudinal and the lateral dynamics.

3.1 Longitudinal dynamics

In the condition of longitudinal dynamics, the study about the car braking starts from the definition of the ideal kinematic equation of the vehicle [13]:

$$v^2 - v^2(0) = 2a_v(t)(x(t) - x(0)) \quad (3.1)$$

Where:

- v: vehicle velocity;
- a: vehicle acceleration;
- x: vehicle position;

The initial conditions in $t = 0$ are the speed v_0 and the position x_0 , which is equal to zero if the reference system is taken on the initial position of the vehicle.

From this equation we can compute the deceleration with reference to the braking space:

$$\Delta x_{target} = (x(t) - x(0)) \quad \text{if we take } x(0) = 0 \implies \Delta x_{target} = x(t)$$

The needed deceleration to stop the vehicle ($v^2(t_{final}) = 0$) is:

$$a_{target} = -\frac{(v^2(0))}{(2\Delta x_{target})} \quad (3.2)$$

The Δx_{target} is also called detection distance $d_{detection}$. To increase the probability to avoid a collision an additional safe distance d_{safe} is added to the computation. Therefore the target deceleration becomes:

$$a_{target} = -\frac{(v^2(0))}{(2(d_{detection} - d_{safe}))} \quad (3.3)$$

An example is the case where a pedestrian crosses the lane in which the vehicle is going as represented in Figure(3.1).

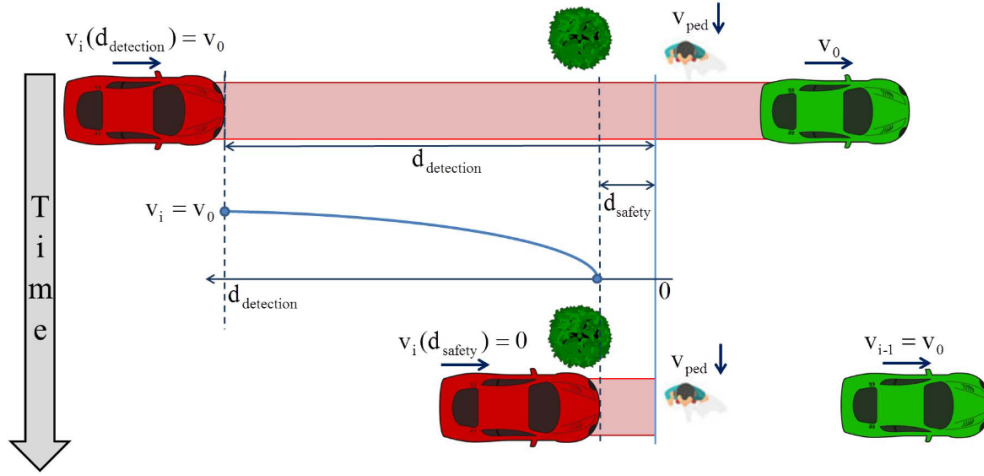


Figure 3.1: Pedestrian crosses the lane [14]

The value of deceleration a_{target} must be smaller in absolute value than the maximum deceleration a_{max} reachable by the vehicle. From this inequality it is possible to compute the minimum detection distance to avoid the collision with a certain initial speed v_0 :

$$|a_{target}| < |a_{max}| \implies d_{detec} = -v_0/(2a_{max}) + 2d_{safe} \quad (3.4)$$

In a dangerous situation, it is necessary to use an emergency braking maneuver to achieve the value of maximum deceleration (or deceleration limit) allowed by the car:

$$|a_{max}| = \mu_{max} \cdot g \quad (3.5)$$

Where g is the gravitational acceleration $\approx 9.81m/s^2$ and μ is the Global Longitudinal Friction Coefficient.

3.1.1 Grip coefficient and Slip Ratio

From the car point of view, μ is the **Grip Coefficient**, which depends on the nature of the tires, the road surface and their general condition (temperature, cleanliness, presence of water, etc.) [15].

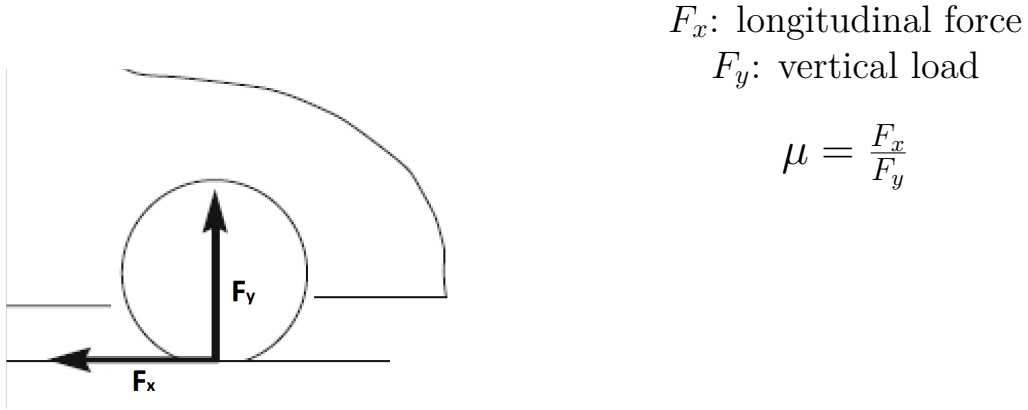


Figure 3.2: Wheel free body diagram

The grip coefficient is strictly related to the **Longitudinal Slip (or Slip ratio)** λ , which measures the wheel slip during the braking manoeuvre and corresponds to the difference between vehicle velocity and the rolling velocity of the tire:

$$\lambda = \frac{(\omega R - v)}{v} \quad (3.6)$$

Where:

- v : vehicle velocity;
- ω : angular speed of the wheel;
- R : rolling wheel radius;

From the equation above two extreme cases can be considered:

1. The first one can occur in presence of icy or snowy road. The vehicle tries to start but the wheels slip and the vehicle's speed remains nil. In this case the wheel angular speed ω can be high but the vehicle speed is equal to zero, so that the slip λ is infinite.
2. When the braking is too hard on a slippery surface (e.g. icy road), the wheels lock, but the vehicle continues to slide forward. In this case the wheel angular speed ω is equal to zero but the vehicle remains in motion and the slip is unitary.

It is possible to define the Grip Coefficient in function of the Longitudinal Slip, using the law $\mu(\lambda)$ in Figure (3.3).

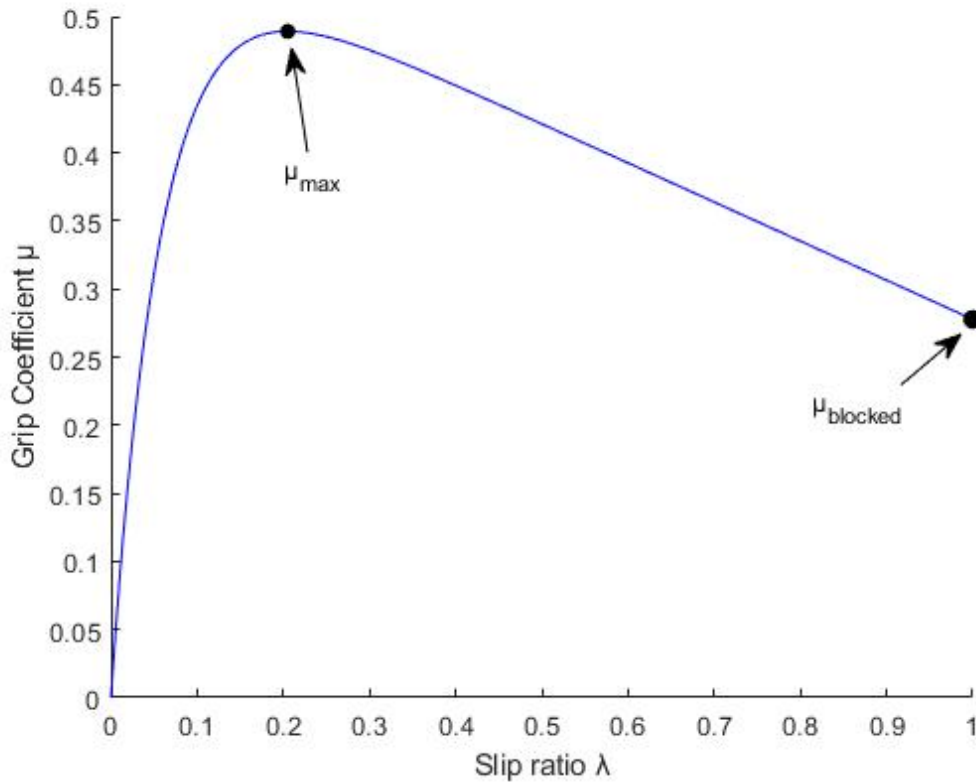


Figure 3.3: Grip Coefficient - Slip Ratio characteristic curve

In the characteristic curve, there are two braking phases divided by the value of the maximum grip coefficient μ_{max} :

- An increase in deceleration, which corresponds to a rise of the friction coefficient to μ_{max} , with a slip rate close to 0.1 (10%). In this phase the harder the driver presses the brake pedal, the more the vehicle decelerates. This is the case of stable braking.
- Then, a deterioration in braking occurs. If the vehicle has no ABS, the coefficient of friction drops from μ_{max} to $\mu_{blocked}$ within approximately 0.2 seconds. In this situation, the wheels lock, λ is equal to 1 and the vehicle skids. This is the case of unstable braking.

In the second point, the wheels locking brings in one of worst possible drive situation: the steering/directional capability is impaired, the grip coefficient decreases while

the braking distance increases, the energy dissipation switches from the brakes to the contact patches and tires get damaged. To avoid these problems, all modern cars are supplied with the ABS (Anti Blocking System or Anti-Lock Braking System).

3.1.2 Burckhardt model

The grip coefficient curve $\mu(\lambda)$ can be estimated using the Burckhardt model [16], that is an analytical model for tire and road behavior based on the Pacejka Magic Formula. The grip coefficient is a function of the slip λ and the vehicle velocity v . The characteristic curve follows:

$$\mu(\lambda, v) = (C_1(1 - e^{(-C_2\lambda)}) - C_3\lambda)e^{(-C_4v)} \quad (3.7)$$

Where:

- C_1 is the maximum value of friction curve;
- C_2 is the friction curve shape;
- C_3 is the friction curve difference between the maximum value and the value at $\lambda = 1$;
- C_4 is the influence parameter of car speed to adhesion, which is in the range 0.02-0.04;

These parameters depend on the road surface conditions and are listed in Table 3.1.

Surface condition	C_1	C_2	C_3	C_4
Dry asphalt	1.029	17.16	0.523	0.03
Wet asphalt	0.857	33.82	0.347	0.03
Dry concrete	1.197	25.168	0.5373	0.03
Snow	0.1946	94.129	0.0646	0.03
Ice	0.05	306.39	0	0.03

Table 3.1: Burckhardt coefficients for different road conditions

The $\mu(\lambda, v)$ curve changes for different vehicle speeds. In Figure (3.4) and Figure (3.5) we can see the corresponding curves for vehicle speed respectively of 10 m/s and 30 m/s .

The five road surface conditions plotted in the two graphics are the ones considered in Table 3.1: dry asphalt (blue), wet asphalt (red), dry concrete (yellow), snow (cyan) and ice (green).

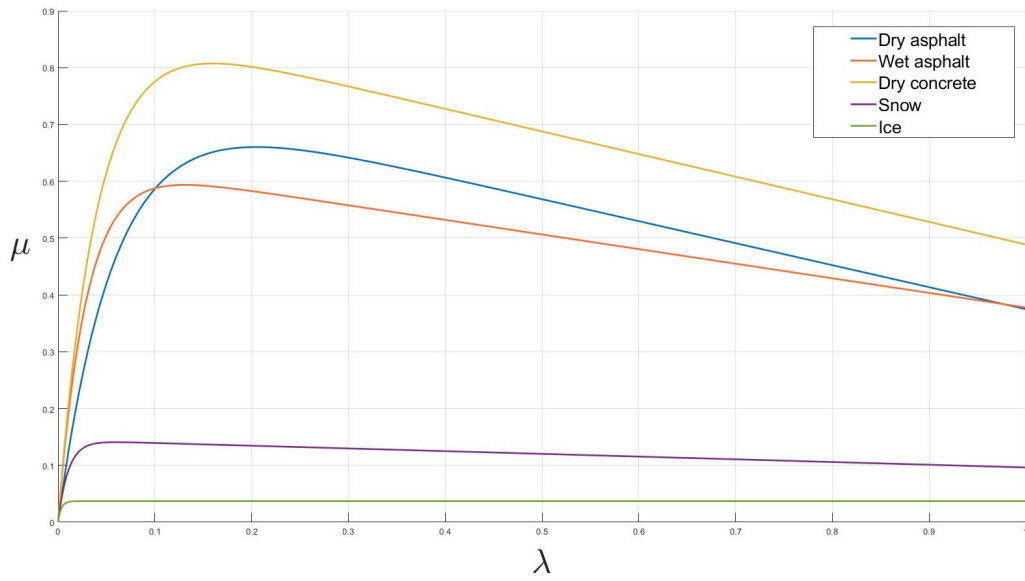


Figure 3.4: Grip coefficient at $v = 10m/s$

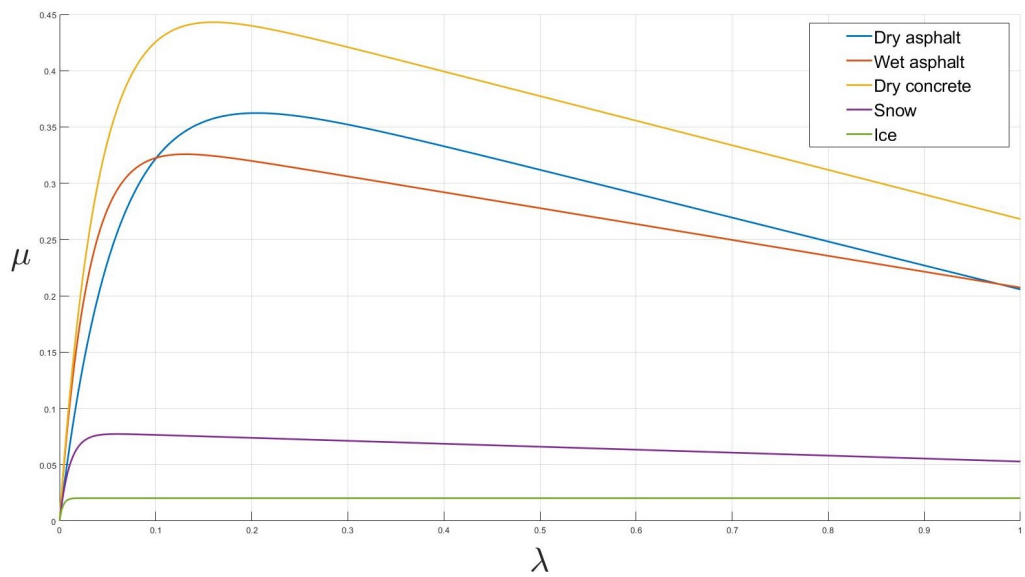


Figure 3.5: Grip coefficient at $v = 30m/s$

Therefore, during a braking manoeuvre, particularly in the emergency braking, it could be useful to have an estimation of the Friction/Grip coefficient and the slip, in order to reach the maximum deceleration allowed by the vehicle and the tire/road contact surface.

3.2 Lateral Dynamics

The lateral dynamics is a crucial case of the braking maneuver (e.g. when the vehicle heads a cornering). There is a higher number of variables and factors to take into account in comparison to the longitudinal case.

The two axis of the car are in different conditions: the rear axis wheels are not modified in position while the front axis are used to change the vehicle direction using the steering wheel. This creates a difference between the direction of the vehicle's motion and the wheel's plane of rotation, called **Slip Angle** δ [grad].

This maneuver brings the vehicle on the effect of a centrifugal force F_c , which tends to force it out of its curve. Therefore, the vehicle generates a centripetal force called **Lateral Force** F_Y equal to F_c .

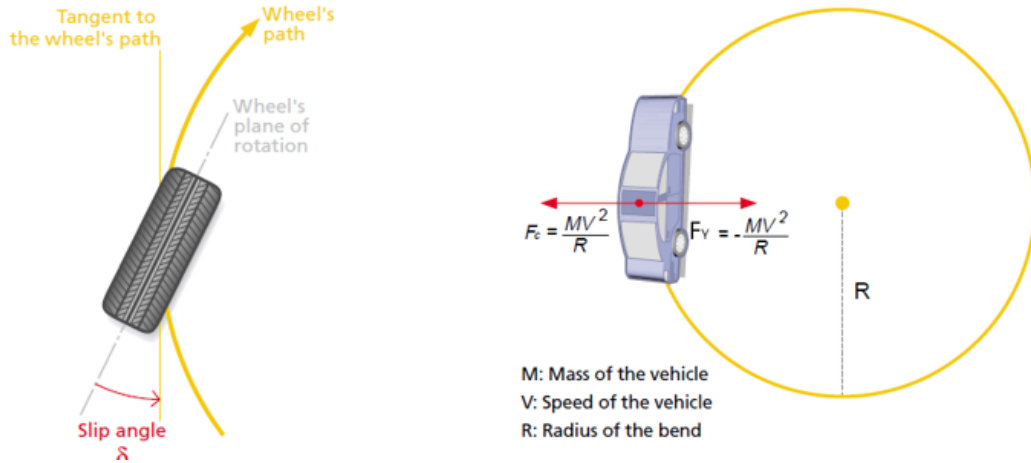


Figure 3.6: Slip Angle and Lateral Force [15]

The **lateral force coefficient** φ can be defined as the relationship between the F_Y and the vertical load F_Z .

This value is equal to the centripetal acceleration devolved by the vehicle's tires and depends on the characteristics of the contact surface:

$$\frac{F_Y}{F_Z} = \varphi \implies F_Y = F_Z \cdot \varphi \tag{3.8}$$

$$\varphi = \ddot{y} \cdot g \text{ and } \ddot{y} = \frac{F_Y}{M} \tag{3.9}$$

The braking and traction dependence of the different longitudinal, lateral and vertical (load) forces can be represented by a graph that uses the longitudinal slip as function argument.

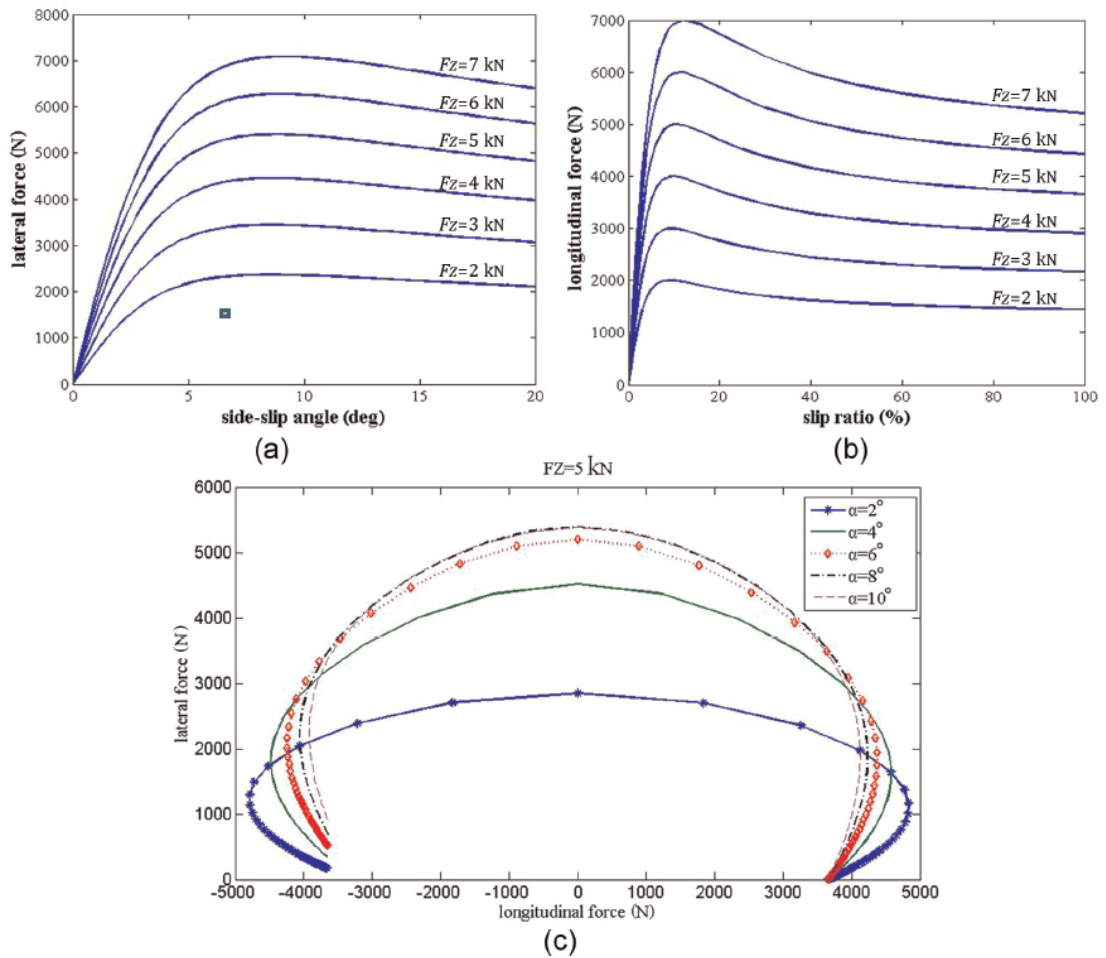


Figure 3.7: (a) lateral force (pure side-slip); (b) longitudinal force (pure longitudinal slip); (c) lateral versus longitudinal force (combined slip) [17]

The graph (C) in the Figure(3.7) shows that the higher the longitudinal force (even when braking), the more lateral force decreases. This phenomenon grows more rapidly for a greater slip angle. For this reason, the consequence of an hard braking is a loss of driveability when cornering.

3.2.1 Kamm circle

The grip of the tyre on the surface is a combination of the longitudinal and lateral grip effort.

The Kamm circle or *friction circle* is used to make a graphical representation of this phenomenon. The maximum value of the two coefficients cannot be reached if both braking and turning are simultaneously present, otherwise there is an occurrence of slippage or loss of driveability.

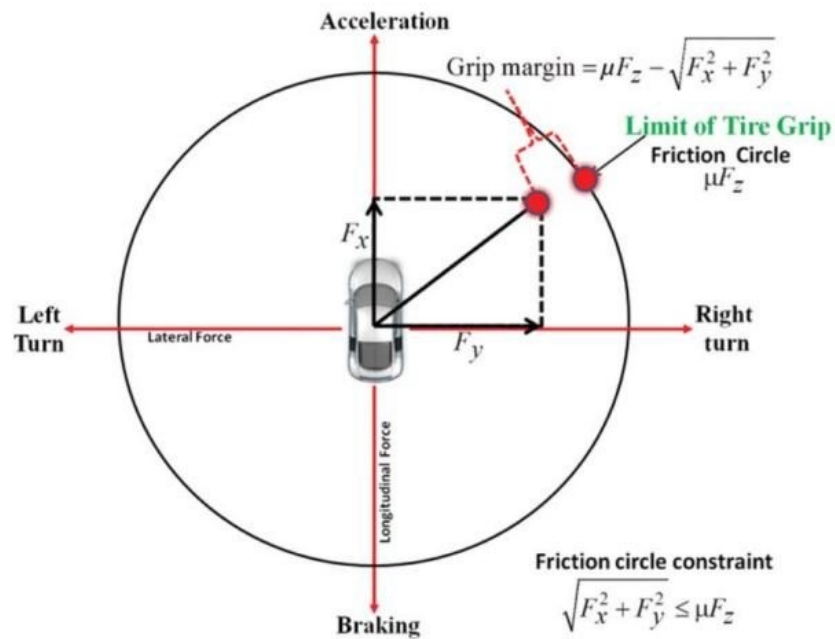


Figure 3.8: Kamm circle [18]

It is possible to conclude that the brakes must be used as less as possible during the turning maneuver. If the brakes are used, the control system must avoid too high leads of lateral force and an increasing of the slip ratio. If the constraints indicated by the Kamm circle are exceeded, it could occur a skid, oversteer or understeer event.

Chapter 4

Model of braking system

A model is a mathematical description of a physical system, but it is an approximation of the real dynamic system, due to the unavoidable uncertainties.

Using “*divide et impera*” (divide and conquer), an old, but gold, roman paradigm, it is developed a model of the car braking system.

This paradigm suggests to divide a complex system into several sub-systems, to have a simple sub-system to be converted directly into a model.

The whole braking system is composed of wheels, brake disc, hydraulic circuit, master cylinder, brake booster and brake pedal. The literature available regarding these elements has been used to generate proper models.

Finally, the modelled sub-systems are combined in a physical model of the whole system.

The braking system model will be useful in the next chapters to estimate the best behaviour, stability and the related requirements of the brake controller.

4.1 Single-Wheel Model

The first step is to find a dynamic model of a single wheel in longitudinal motion, in which a Brake Torque T_b is applied.

Starting from the free-body diagram in Figure (4.1), we can derive a longitudinal vehicle model considering the rotational dynamics of the wheel.

A car has four wheels that should be studied separately, to obtain a more accurate model. On the other hand, the system designed in this thesis will be not able to control the braking force distribution on the four wheels.

Due to this limitation, in this project a generic single wheel model is enough to study the braking system.

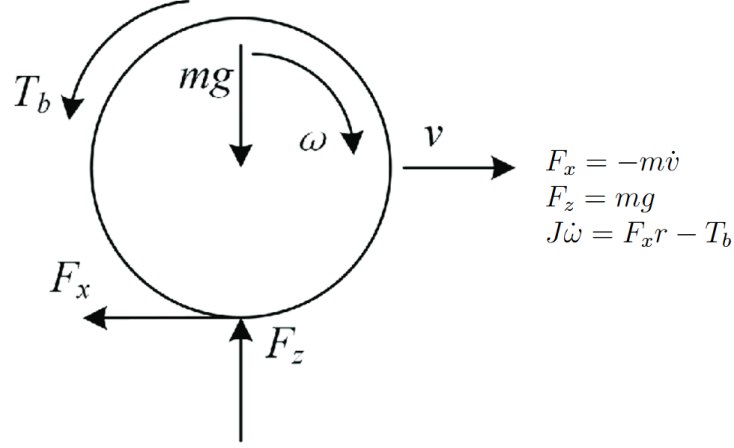


Figure 4.1: Single-wheel free-body diagram [19]

The elements present are:

- m : quarter mass vehicle [kg];
- g : gravitational acceleration [m/s^2];
- r : wheel radius [m];
- ω : wheel angular speed [rad/s];
- J : polar moment of inertia of the wheel;
- Inertia Ratio: $\tau_J = \frac{mr^2}{J}$ [kgm^2];

The value of Longitudinal Force F_x is computed considering the grip coefficient μ_x estimated using the Buckhardt model in Section 3.1.2.

$$F_x = \mu_x \cdot F_z \quad (4.1)$$

where $\mu_x = \mu(\lambda, v) = (C_1(1 - e^{(C_2\lambda)}) - C_3\lambda)e^{(-C_4v)}$.

The value of the speed v and the longitudinal slip λ are taken as dynamic states, so it's possible to find the state equation:

$$\begin{cases} F_x = -m\dot{v} = \mu(\lambda, v) \cdot m \cdot g \\ \dot{\omega} = \frac{\mu(\lambda, v)mgr - T_b}{J} \\ \lambda = \frac{v - \omega r}{v} \end{cases} \quad \begin{cases} \dot{v} = -m\mu(\lambda, v) \\ \dot{\lambda} = -\frac{\dot{\omega}r}{v} + \frac{\omega r}{v^2}\dot{v} \\ \omega = \frac{v}{r}(1 - \lambda) \end{cases} \quad (4.2)$$

$$\begin{cases} \dot{v} = -m\mu(\lambda, v) \\ \dot{\lambda} = -\frac{g}{v} \left(\frac{\mu(\lambda, v)mr^2 - \frac{T_b r}{g}}{J} \right) - \frac{(1-\lambda)\mu(\lambda, v)g}{v} \end{cases} \quad (4.3)$$

$$\begin{cases} \dot{v} = -m\mu(\lambda, v) \\ \dot{\lambda} = -\frac{g}{v} (\mu(\lambda, v)((1-\lambda) + \frac{mr^2}{J}) + T_b \frac{r}{Jv}) \end{cases} \quad (4.4)$$

Using these equations, we can define a state-space model of the dynamic system:

$$\begin{aligned} \text{State: } x(t) &= \begin{bmatrix} x_1(t) \\ x_2(t) \end{bmatrix} = \begin{bmatrix} v(t) \\ \lambda(t) \end{bmatrix} & \lambda \in [0,1] \text{ and } v \in \mathbb{R}^+ \\ \text{Input: } u(t) &= T_b & T_b : \text{Brake Torque} \in \mathbb{R}^+ \\ \text{Output: } y(t) &= x_1(t) = v(t) & v : \text{Vehicle speed} \in \mathbb{R}^+ \end{aligned}$$

$$\text{State equation: } \begin{bmatrix} \dot{x}_1(t) \\ \dot{x}_2(t) \end{bmatrix} = \begin{bmatrix} -m\mu(x_2, x_1) \\ -\frac{g}{x_1} (\mu(x_2, x_1)(1-x_2) + \tau_J) + u \frac{r}{Jg} \end{bmatrix} \quad (4.5)$$

The elements in the state equation are:

- m: quarter mass vehicle [kg];
- g: gravitational acceleration [m/s²];
- r: wheel radius [m];
- w: wheel angular speed [rad/s];
- J: polar moment of inertia of the wheel [m⁴];
- Inertia Ratio: $\tau_J = \frac{(mr^2)}{J}$ [kg/m²];

The dimensions of the system are $n_x = 2$, $n_u = 1$ and $n_y = 1$, therefore it can be considered a SISO system.

4.2 Disc Brake

The disc brake device is composed by one piston where the hydraulic pressure is converted to the forces applied to the pads.

The contact between the pads and the disc makes a friction force that is used to have the brake torque on the wheel.

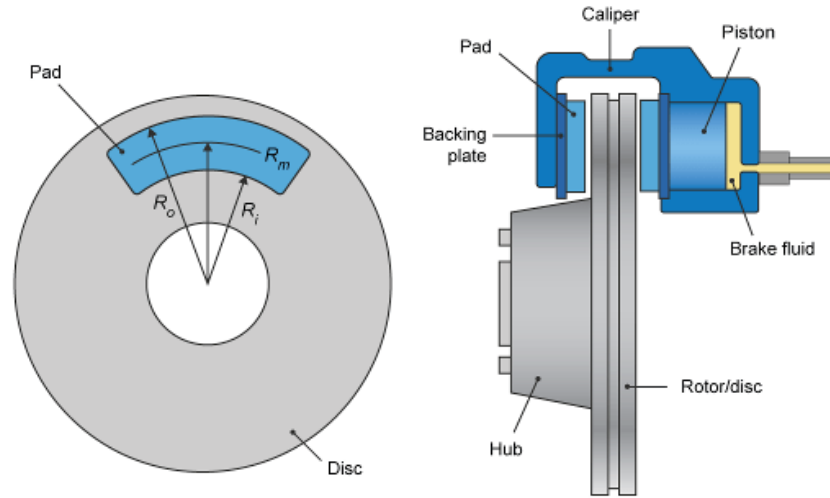


Figure 4.2: Disc brake components [20]

This dynamic system is defined with the following equations:

$$\begin{cases} F_p = A_p \cdot P_{mc} \\ F_{pad} = N \cdot F_p \\ F_b = F_{pad} \cdot \mu_{disc} \\ T_b = F_b \cdot R_m \end{cases} \quad (4.6)$$

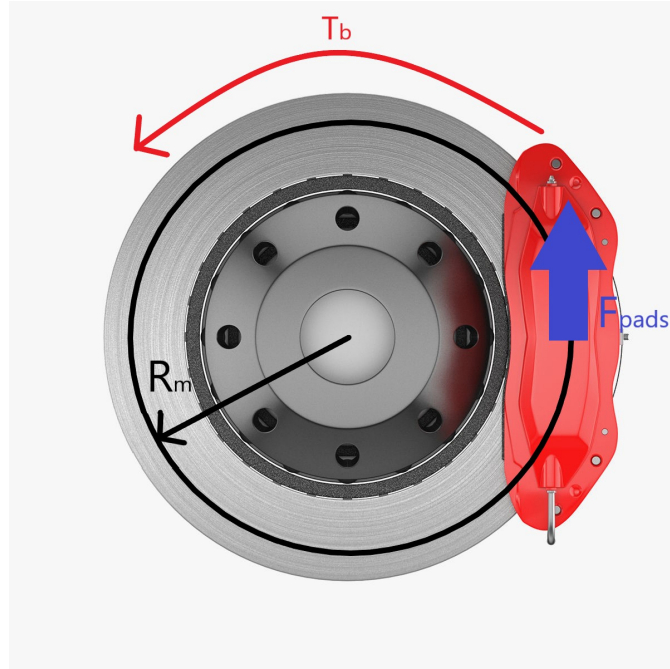


Figure 4.3: Disc brake free-body diagram

The elements of the system are:

- P_{mc} : the pressure applied on the piston which is connected to the master cylinder by the brakes line [Pa];
- A_p : the area of the piston [m²];
- F_p : the force provided by the piston on the pads [N];
- N : the number of brake pads in disc brake assembly;
- F_{pad} : the normal force on the disc, which is applied by two pads on the disc [N];
- μ_{disc} : the disc-pads coefficient of kinetic friction;
- F_b : the tangential force to the disc, which is provided by the friction between disc and pads [N];
- R_m : the radius between the center of the wheel and the point where the braking force [m] is applied;

Finally, the brake torque equation becomes:

$$T_b = N \cdot A_p \cdot P_w \cdot \mu_{disc} \cdot R_m \quad (4.7)$$

The disc-pad coefficient μ_{disc} is a value depending on the surface materials characteristics and conditions.

The related disc abrasive wear depends on the time of usage, the ambient atmospheric conditions, as humidity and temperature and other factors.

It is possible to approximate it to a value ≈ 0.38 in the normal conditions [21].

4.3 Brake Hydraulic System

The brake hydraulic system provides the connection between user-side and the disc brake side using the pressure of the hydraulic fluid (typically an oil based on glycol ether) inside the system.

The system described above is the most used in common cars, whose components are described in the following Subsections.

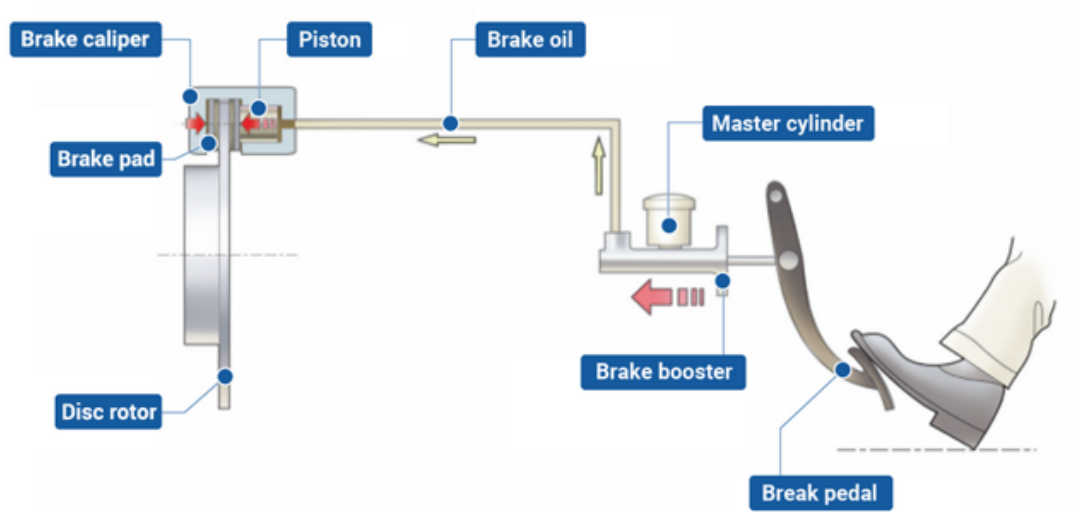


Figure 4.4: Whole brake system [22]

4.3.1 Master Cylinder

The master cylinder, sometimes called Tandem Master Cylinder (TMC), converts the input force provided from the brake booster in a pressure and carries it in the different wheel cylinder.

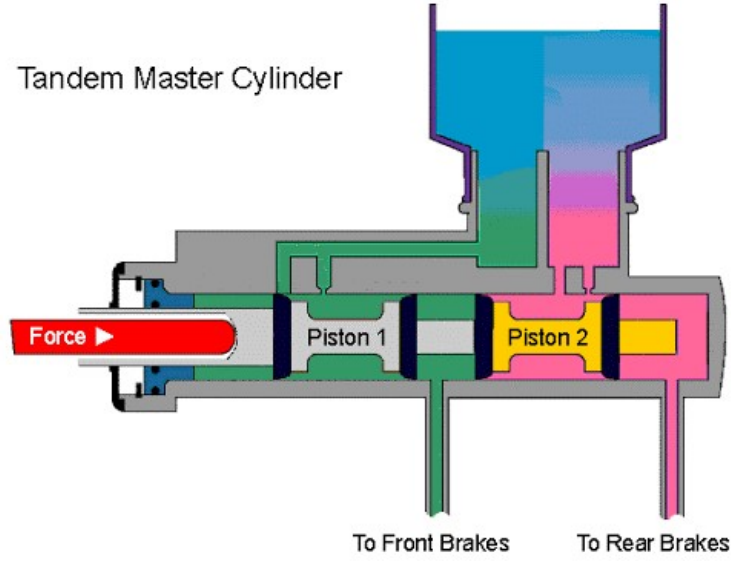


Figure 4.5: TMC [23]

The TMC has two independent fluid circuits for each couple of wheels so that it makes the braking system redundant.

In case of a leakage or a failure inside one of brake lines, the other is not compromised and the braking manoeuvre is still possible with a loss in the performance.

The system can be simplified in a model in which the outlet pressure in the two lines is equal. The value of the inner pressure depends on the force applied on the input TMC rod and the area of the pistons.

The equations of the system are:

$$\begin{cases} P_{mc} = F_{out,booster} / A_{mc} \\ P_{mc} = P_{fb} = P_{rb} = P_w \\ F_{fp} = P_{mc} \cdot A_{fp} \\ F_{rp} = P_{mc} \cdot A_{rp} \end{cases} \quad (4.8)$$

Therefore, the rear and front brakes can have different braking forces. The ratio between them is defined as:

$$\text{Front-Rear brake ratio: } \eta_{fr} = \frac{F_{fp}}{F_{rp}}$$

This value is often greater than one because it is better to have a greater braking force in the front brake.

A locking of the rear wheels is more dangerous, because it can bring to an oversteering event, which is more unstable than an understeering one.

4.3.2 Brake circuit

The brake circuit is composed by pipes and hoses, which carry the brake oil pressure from the TMC to the brake disk device.

The brake circuit architecture can have multiple forms: common cars use the "X" or "II" configuration depending on which wheels have the same independent line.

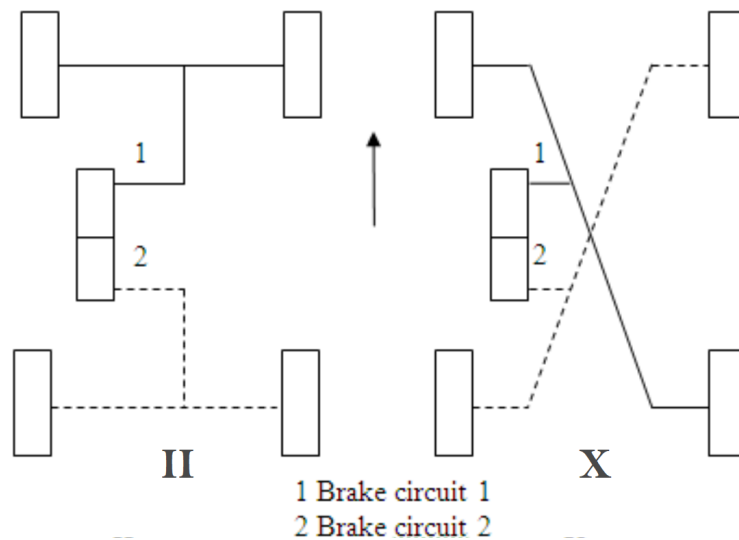


Figure 4.6: X and II brake circuit configurations

4.3.3 Brake booster

The brake booster is a device that amplifies the pedal force and is useful to reduce the effort required by the user to reach the target deceleration. There are different types of boosters on the market, but they work in a similar way.

The most common way is the vacuum booster, which utilizes the negative pressure to amplify the input force. This kind of device is present in the vehicle analyzed in this study, but also there are some changes due to the full electric power unit.

4.3.4 Brake vacuum booster + TMC

The use of data collected from a real braking system allows to find a characteristic curve that considers the actions of the vacuum booster and the TMC.

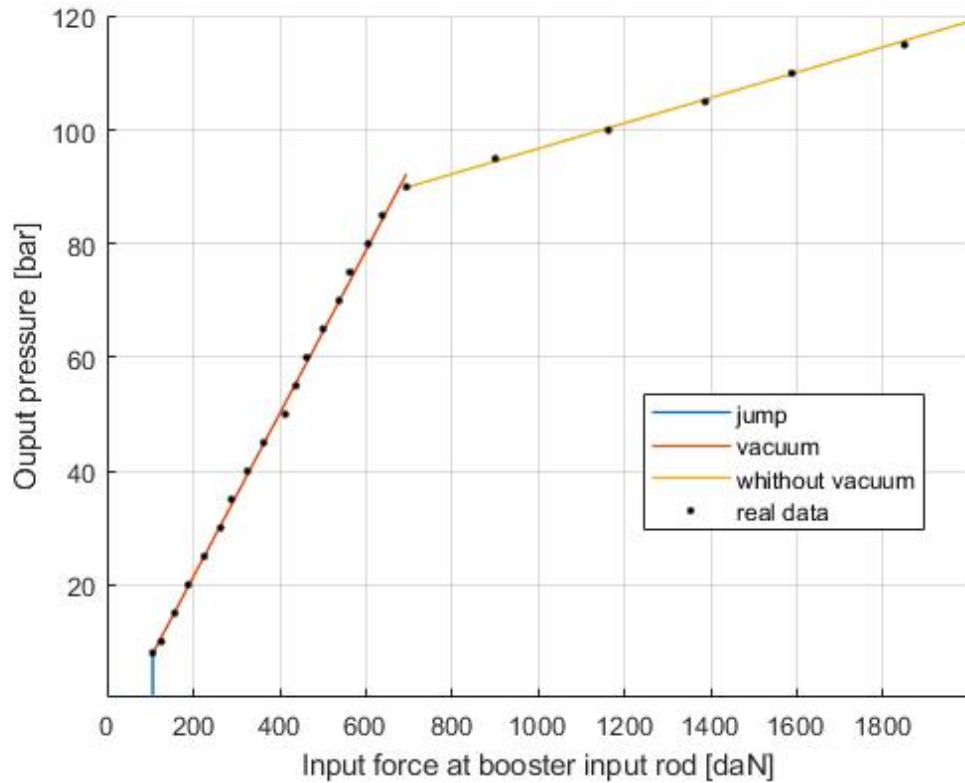


Figure 4.7: Characteristic diagrams curves at ambient temperature

Figure (4.7) shows the relationship between the input force at booster input rod and the output pressure in the brake circuit.

It is possible to observe that for an applied force under the *Crack point* equal to 10.5 daN the pressure is equal to 0.

After this threshold value there is a *Jump-in* of outlet pressure: this is due to the push-out pressure that requires a minimum effort to produce an output pressure in TMC. In this situation, the disc and the pads are in contact, there is a deceleration and the curve becomes linear with slope K_{b1} .

The last threshold is called *Knee point* and after this value of input force the booster ends to amplify due to its physical limitation.

The new slope K_{b2} is quite similar to the case of the booster without vacuum.

Therefore, the coefficient of the characteristic curve can be defined as:

$$K_b = \begin{cases} 0 & \text{if } F_{in} < 10.5\text{daN} \\ K_{b1} & \text{if } 10.5\text{daN} \leq F_{in} \leq 65\text{daN} \\ K_{b2} & \text{if } F_{in} > 65\text{daN} \end{cases} \quad (4.9)$$

The value of the two slopes (K_{b1}, K_{b2}) is computed with the method of least squares, using the data provided by the component supplier in the characteristic curve.

The value of the brake pressure can be expressed as:

$$P_{mc} = F_{in} \cdot K_b \quad (4.10)$$

4.3.5 Pedal

The pedal is usually used by the driver to control the vehicle deceleration with a force applied to its tip.

It can be considered a suspended second-class lever.

The free-body diagram is shown in Figure 4.8.

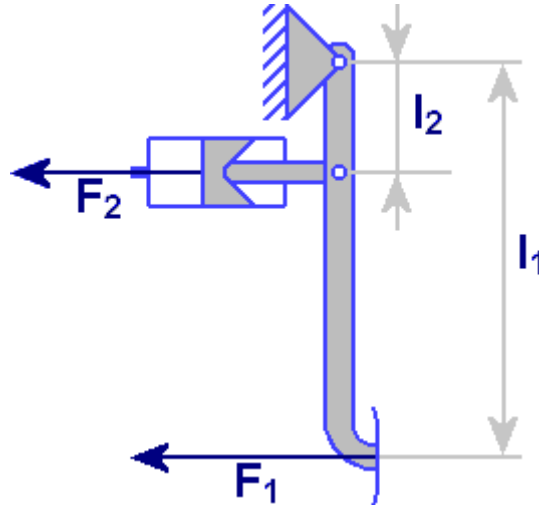


Figure 4.8: Pedal free-body diagram [24]

The **pedal ratio** is the multiplicative factor between the input pedal force F_1 and the output force $F_2 = F_p$.

The output force pushes on the rod connected to the booster input:

$$\tau_{pedal} = \frac{l_1}{l_2} \implies F_2 = F_1 \cdot \tau_{pedal} \quad (4.11)$$

The tests carried out on the vehicle provide a pedal force corresponding to pedal stroke characteristic, which is useful to have a control of deceleration by mean of the movement of the pedal position.

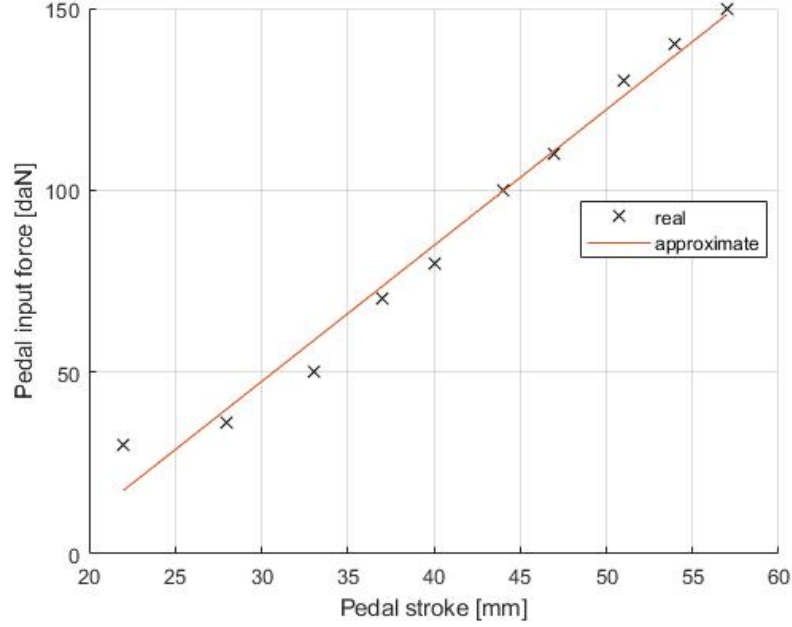


Figure 4.9: pedal force – pedal stroke characteristic

The least squares method is used to find the coefficient of the approximate curve K_p . Therefore, the force applied on the booster input is equal to the pedal position x_p multiplied to the coefficient K_p :

$$F_p = x_p \cdot K_p \implies K_p = \frac{F_p}{x_p} \quad (4.12)$$

This relationship is valid only for values greater than the free travel threshold $\approx 22 \text{ mm}$. The pedal has a full-scale value depending on the pedal mechanical design.

4.4 Whole Braking System

Given the braking system devices and their models discussed in the previous Sections, it is possible to define the complete brake model, that can be simplified in a single braking gain G_b .

The braking gain is defined as the relationship between the pedal travel and the brake torque applied on the wheel.

Input: pedal position x_{pedal} [mm]

Output: brake torque T_b [N m]

$$\begin{cases} T_b = 2A_p \cdot P_w \cdot \mu_{disc} \cdot R_m \\ P_w = F_{in,mc} \cdot Kb \\ F_{in,mc} = x_p \cdot K_p \end{cases} \implies T_b = 2A_p \cdot \mu_{disc} \cdot R_m \cdot K_b \cdot K_p \cdot x_p \quad (4.13)$$

Then:

$$G_b = \begin{cases} 0 & \xrightarrow{\text{if}} F_{in} < 10.5\text{daN} \\ 2A_p \cdot \mu_{disc} \cdot R_m \cdot K_{b1} \cdot K_p & \xrightarrow{\text{if}} 10.5\text{daN} \leq F_{in} \leq 65\text{daN} \\ 2A_p \cdot \mu_{disc} \cdot R_m \cdot K_{b2} \cdot K_p & \xrightarrow{\text{if}} F_{in} > 65\text{daN} \end{cases} \quad (4.14)$$

$$T_b = G_b \cdot x_p \quad (4.15)$$

This compact form is added to the single wheel model taking as input the pedal stroke x_p and adding the braking gain in the state equations:

$$\begin{aligned} \text{State: } x(t) &= \begin{bmatrix} x_1(t) \\ x_2(t) \end{bmatrix} = \begin{bmatrix} v(t) \\ \lambda(t) \end{bmatrix} & \lambda \in [0,1] \text{ and } v \in \mathbb{R}^+ \\ \text{Input: } u(t) &= x_p & x_p : \text{Pedal stroke} \in [0, x_p^{max}] \\ \text{Output: } y(t) &= x_1(t) = v(t) & v : \text{Vehicle speed} \in \mathbb{R}^+ \end{aligned}$$

$$\text{State equation: } \begin{bmatrix} \dot{x}_1(t) \\ \dot{x}_2(t) \end{bmatrix} = \begin{bmatrix} -m\mu(x_2, x_1) \\ \frac{g}{x_1}(\mu(x_2, x_1)((1 - x_2) + \tau_J) + uG_b \frac{r}{J_g}) \end{bmatrix} \quad (4.16)$$

Chapter 5

Design of Braking Actuator System

5.1 Design contest

The car Citroën e-Méhari has been modified to have an autonomous driving system with the aim to reach the SAE level 3. Therefore, the braking system needs to have an Advanced Driver Assistance Systems (ADAS).

The idea is to use the actuator system designed to replace the action of the driver foot on the brake pedal. The actuation will be controlled by a proper Electronic Control unit (ECU).

The main actuator is a servo DC motor, which is able to provide a certain value of torque and speed. The critical points to use this kind of motor device for this project purpose are:

1. The nominal motor torque is lower than the maximum torque required by the braking system;
2. The resolution to control the motor is too low, due to a too small full-range;
3. The mechanical motion provided by the motor is angular, while the pedal needs a linear motion;
4. The size of the motor requires a displacement from the brake pedal;

The first two problems are solved with the addition of a gear-box, in such way the nominal torque is increased and the speed is decreased. The speed decrease allows to improve the sensibility, so that the motor full-scale is multiplied by the gear-box ratio.

The solution of the third problem is the design of a proper system, composed by a

lever (or rods/rib) to convert the different typologies of motion.

It is also useful to additionally increase the value of force and to decrease the speed of the motor.

The fourth problem can be solved using a Bowden rope, which is a good trade-off between flexibility and capability to transmit mechanical force.

This rope solution allows to install the motor in a different position, chosen taking into account the user's comfort and the assembly constraints.

5.2 Mechanical Model

A simple free-body diagram of the mechanical system has been drawn on Figure (5.1) to define the system dynamic.

All the physical elements between the DC motor to the brake pedal are considered.

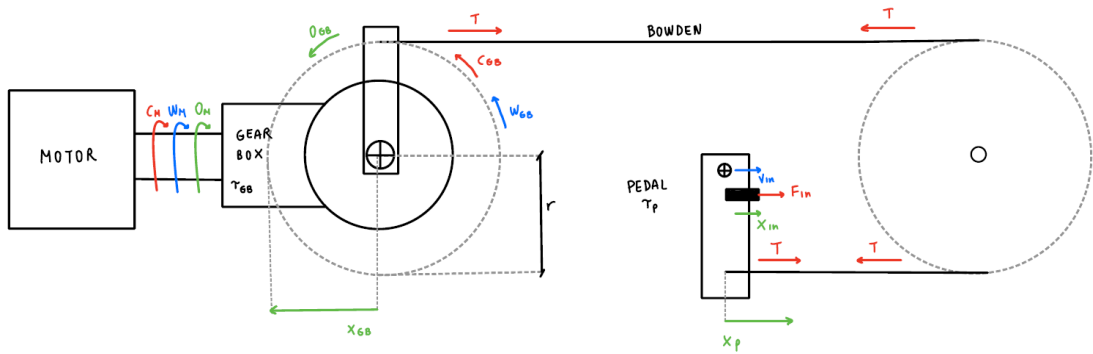


Figure 5.1: Mechanical actuator free-body diagram

The equations describing the system are:

$$F_{IN} = \frac{C_M}{r} \cdot \tau_{GB} \cdot \tau_P \quad (5.1)$$

$$v_{in} = \omega_M \cdot r \cdot \frac{1}{\tau_{GB}} \cdot \tau_P \quad (5.2)$$

$$x_P = x_{GB} = x_{IN} \cdot \tau_P \quad (5.3)$$

$$\theta_{GB} = \frac{x_{GB}}{r} \cdot \frac{180}{\pi} \quad (5.4)$$

Where:

- C_M : Nominal torque of motor [N m];
- ω_M : Nominal angular speed of motor [rad m];
- θ_M : Angular position of the motor shaft [rad];
- τ_{GB} : Ratio of gear box;
- C_{GB} : Torque of gearbox [N m];
- ω_{GB} : Angular speed of gearbox [rad/s];
- θ_{GB} : Angular position of the gearbox shaft [rad];
- r : Radius of the rod used to convert the angular motion in linear motion [m];
- x_{GB} : Displacement of the Bowden rope in the GB side [m];
- x_P : Displacement of the Bowden rope in the pedal side [m];
- τ_P : Ratio of pedal;
- F_{in} : Force of the input booster rod [N];
- v_{in} : Speed of the input booster rod [m/s];
- x_{in} : Displacement of the input booster rod [m];
- M_{cycle} : Motor cycles;

The choice of the components of the whole system is done considering the worst working condition:

- F_{in} must be greater than the maximum force required by the booster;
- v_{in} must be fast enough to provide the best braking response;
- θ_{GB} must be maximum 45° to remain in a small angle condition;
- x_P must have a full-range compatible with the pedal one;
- M_{cycle} must be maximized to have the best sensibility in the motor control;

The model studied in the previous Chapter needs another change: the input pedal travel is no longer the input of the state equations but the angular position of the brushless DC motor. The new input is added using the actuation gain G_a , which puts in relationship θ_M and the pedal stroke x_p :

$$G_a = \frac{r}{\tau_{GB}} \implies x_p = G_a \cdot \theta_M \quad (5.5)$$

Therefore, the new system is defined as:

$$\begin{aligned} \text{State: } x(t) &= \begin{bmatrix} x_1(t) \\ x_2(t) \end{bmatrix} = \begin{bmatrix} v(t) \\ \lambda(t) \end{bmatrix} && \lambda \in [0,1] \text{ and } v \in \mathbb{R}^+ \\ \text{Input: } u(t) &= \theta_m && \theta_m : \text{motor angular position} \in [0, \theta_m^{max}] \\ \text{Output: } y(t) &= x_1(t) = v(t) && v : \text{Vehicle speed} \in \mathbb{R}^+ \end{aligned}$$

$$\text{State equation: } \begin{bmatrix} \dot{x}_1(t) \\ \dot{x}_2(t) \end{bmatrix} = \begin{bmatrix} -m\mu(x_2, x_1) \\ -\frac{g}{x_1}(\mu(x_2, x_1)((1-x_2) + \tau_J) + uG_aG_b\frac{r}{Jg}) \end{bmatrix} \quad (5.6)$$

5.3 Servo DC motor

The motor system is composed by an electrical part and a mechanical part. Using the fundamental laws of their respective domains, it is possible to find a model that considers both characteristics [25].

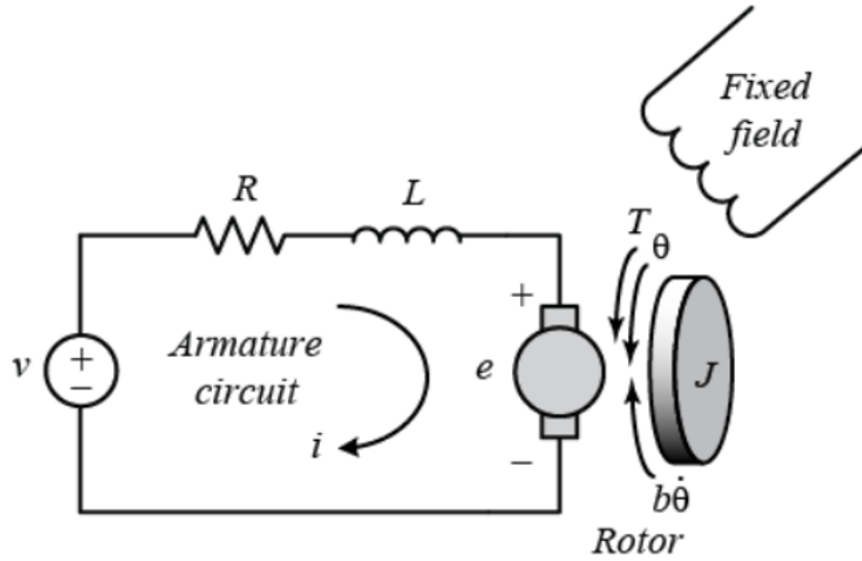


Figure 5.2: Servo DC motor equivalent circuit

The equation used to describe the DC motor are based on the Newton's 2nd law and Kirchhoff's voltage law.

$$\begin{cases} J\ddot{\theta} + b\dot{\theta} = Ki \\ L\frac{di}{dt} + Ri = V - K\dot{\theta} \end{cases} \quad (5.7)$$

$$\text{In state space form: } \frac{d}{dt} \begin{bmatrix} \dot{\theta} \\ i \end{bmatrix} = \begin{bmatrix} -\frac{b}{J} & \frac{K}{J_R} \\ \frac{K}{L} & -\frac{R}{L} \end{bmatrix} \cdot \begin{bmatrix} \dot{\theta} \\ i \end{bmatrix} + \begin{bmatrix} 0 \\ \frac{1}{L} \end{bmatrix} V \quad (5.8)$$

Where:

J : Rotor Inertia [$\text{kg} \cdot \text{m}^2$];

R : equivalent resistance of the motor [Ω];

L : equivalent inductance of the motor [H];

θ : angular speed of the motor [rad/s];

i : current flow in the motor armature [A];

V : input motor voltage [V];

K_e : back-EMF (electric motor force) constant;

K_t : motor torque constant;

$K = K_t = K_e$ is a common approximation;

This system can be represented in a frequency domain as a LTI second-order transfer function, in which the input is V and the output is θ :

$$G(s) = \frac{\dot{\theta}(s)}{V(s)} = \frac{K}{(Js + b)(Ls + R) + K^2} \quad (5.9)$$

The motor device is a modular system composed by the motor and a feedback control loop to reach and maintain the target angle position. The motor is design to work without the addition of further control system.

The servo motor is a particular case of DC motor, is can be defined as rotary actuator that allows using a signal control, as a duty cycle of an input PWM signal, to have a precise control of angular position, acceleration, and velocity.

The motor is an electromechanical system with an integrated sensor for position feedback.

In terms of the model is possible to simplified as the stable first order transfer functions G_{servo} in (5.10).

$$G_{servo}(s) = \frac{1}{\tau_{servo}s + 1} \quad (5.10)$$

The Servo DC motor time constant (time lag) is take from the component data-sheet $\tau_{servo} \approx 0.2$.

Chapter 6

Control system design

The braking system is one of the most critical devices in the vehicle, for this reason it requires to have stability, robustness, precision and speed of response.

In the state-of-art, the system designed is an open-loop system, which is not able to satisfy the autonomous system requirements.

The solution is to implement a close-loop control system, using a proper control law, in order to minimize the error from the reference target value provided by the autonomous driving system.

The upper level controller is designed to control in speed the vehicle in deceleration phase, indeed the goal is to minimize the error between the vehicle speed target and real vehicle speed.

The control to design is a MISO system, with dimensions: $n_{in} = 2$ $n_{out} = 1$: The controller inputs are:

1. The target speed v_r , which is provided by the autonomous driving unit;
2. The slip ratio λ , which will be used to modulate the braking effort, to avoid the skidding of the vehicle;

The controller output is:

1. The target angular position θ_M of the motor shaft, as showed in the previous pages;

6.1 Block diagrams

The whole system can be represented in a block diagram in this way:

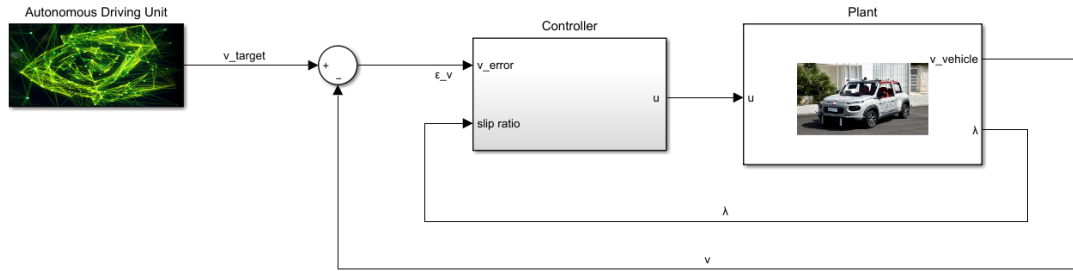


Figure 6.1: Whole system Matlab block diagram

The plant is composed by the servo motor, the vehicle braking system and the single wheel model. The block diagram inside is:

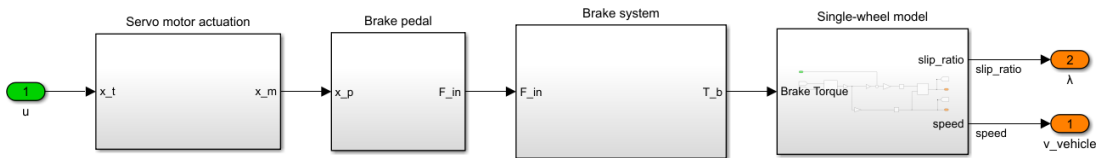


Figure 6.2: Plant block diagram

The servo motor can be considered as a stable first order transfer function, with a delay τ_m , as discussed in section 5.3.

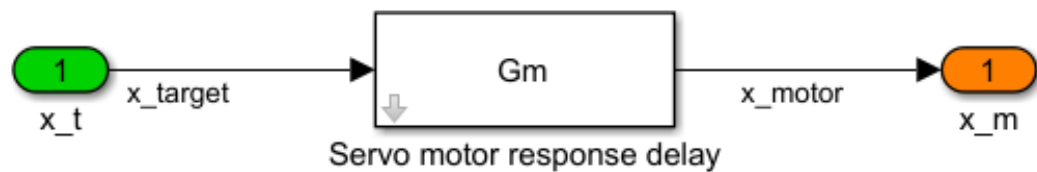


Figure 6.3: Servo motor block diagram

The gains K_b and K_p defined in (4.9) and (4.12) are implemented as two look-a-table.

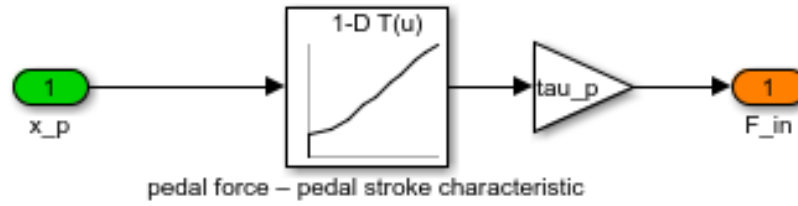


Figure 6.4: Pedal block diagram

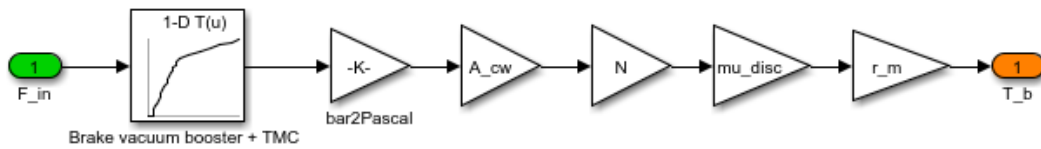


Figure 6.5: Brake system block diagram

The last but not least element in the plant block is the single wheel model, that includes the physics model of the wheel, which has been discussed in Section 4.1. It estimates the behavior of the vehicle motion under the effort of brake torque and road surface condition.

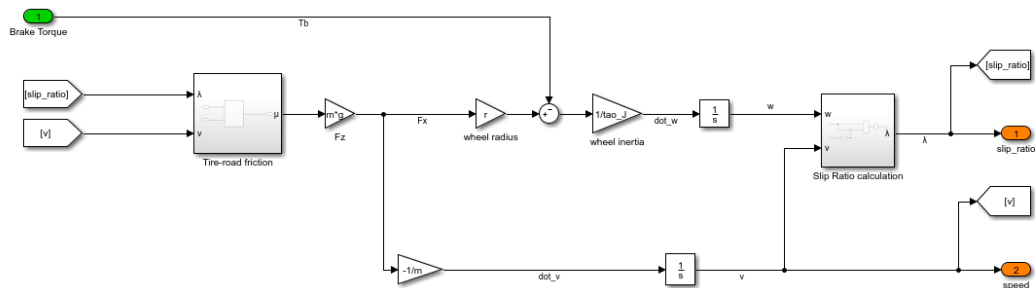


Figure 6.6: Single-wheel model block diagram

6.2 Model Analysis

The model obtained in the previous chapters is a Nonlinear and Time-invariant system.

In literature there are many studies about the equilibrium point and the stability of the single wheel model, defined by the differential equations:

$$\begin{cases} \dot{v} = -m\mu(\lambda, v) \\ \dot{\lambda} = -\frac{g}{v}(\mu(\lambda, v)((1 - \lambda) + \frac{mr^2}{J}) + Tb\frac{r}{Jv}) \end{cases} \quad (6.1)$$

The domains of the two states are:

- Longitudinal Slip: $\lambda \in [0, 1]$
- Vehicle speed: $v \in [0, +\infty)$

6.2.1 Equilibrium points

Assuming that the input θ_M is constant (or slowly changing) and $x_p > 22mm$, the system can be considered as a second-order autonomous system. In the study of the breaking, the case $\dot{v} = 0$ in which the speed is constant is meaningless. Therefore, as discussed in [26] the equilibrium points of this model is interesting only for $\dot{\lambda} = 0$ characteristic.

We can study the equilibrium point with a first-order model of the single wheel system, with the assumption that the Brake Torque is $T_b > 0$ and that the vehicle speed is slowly-changing.

Using the expression $v = \frac{\omega}{r}(1 - \lambda)$, the (6.1) become:

$$\dot{\lambda} = -\frac{1 - \lambda}{J\omega} \left(r + \frac{J}{rm}(1 - \lambda) \right) mg\mu(\lambda) - T_b \quad (6.2)$$

For simplicity:

$$\Psi(\lambda) = \left(r + \frac{J}{rm}(1 - \lambda) \right) mg\mu(\lambda) \quad (6.3)$$

Then with $\omega > 0$:

$$\dot{\lambda} = -\frac{1 - \lambda}{J\omega} (\Psi(\lambda) - T_b) \quad (6.4)$$

From this last equation it is easy to say that the equilibrium points are found for:

$$\bar{T}_b = \Psi(\bar{\lambda}) \quad (6.5)$$

This means that for a constant control input can exist two condition in terms of equilibrium points:

1. If $\bar{T}_B > \max(\Psi(\lambda))$, the system has **no equilibrium point**, recall that the model has been derived under the assumption that $\theta \in [0, 1)$;
2. If $\bar{T}_B \leq \max(\Psi(\lambda))$, the system has **at most two equilibrium point**, namely λ_a and λ_r in Figure (6.7), where $\lambda_a \leq \lambda_r$ are the two possibly coincident solutions of

$$\bar{T}_b = \Psi(\bar{\lambda})$$

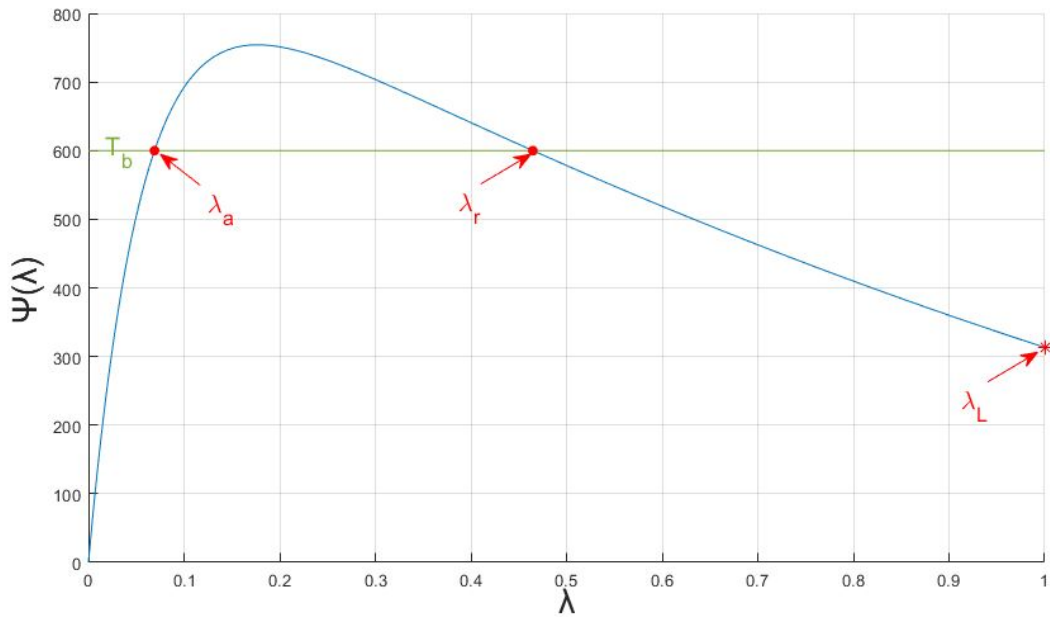


Figure 6.7: Equilibrium points for the single wheel model (6.1) in the (λ, T_b) plane (example with dry asphalt)

If $\lambda = 1$ is considered also acceptable, there is an additional eq. point, that is completely locked wheels, then (6.4) clearly shows that λ_L implies $\dot{\lambda} = 0$ for all values of the braking torque T_b , which means that the condition of locked wheels is an equilibrium point for the system. This means that the presence of the two equilibrium points depends on the braking torque, which is related to the angle of the servo motor $T_b = G_a G_b \theta_M$.

6.2.2 Model Linearization and Stability Analysis

Using the first-order nonlinear system (6.1), the stability properties of the equilibrium points can be investigated by analysing the behaviour of the open-loop vector

field in the case $\bar{T}_B \leq \max(\Psi(\lambda))$.

Consider now the following variables defined around an equilibrium point (characterised by T_b, λ):

$$\delta T_b = T_b - \bar{T}_b; \quad \delta \lambda = \lambda - \bar{\lambda} \quad (6.6)$$

To carry out the linearization of the system, a crucial issue is how to consider and manage the dynamic dependency on the variable v . Often, a simple quasi-static assumption is made: v is assumed to be a slowly-varying parameter since it is assumed that the longitudinal dynamics of the vehicle are much slower than the rotational dynamics of the wheel. As such, to linearize the model, the simplest approach is to work with the first-order model of the single wheel dynamics [4.4] and neglect the equation $\dot{v} = -m\mu(\lambda, v)$.

To do this, it is needed to define the slope of the $\mu(\lambda)$ curve around the equilibrium point:

$$\mu_1(\bar{\lambda}) := \left. \frac{\delta \mu}{\delta \lambda} \right|_{\lambda=\bar{\lambda}} \quad (6.7)$$

The friction curve $\mu(\lambda)$ can now be expressed around the equilibrium point $\bar{\lambda}$ as:

$$\mu(\lambda) \approx \mu(\bar{\lambda}) + \mu_1(\bar{\lambda})\delta\lambda \quad (6.8)$$

Therefore, assuming a constant speed $v = \bar{v}$ the linearized single wheel model :

$$\delta \dot{\lambda} = \frac{F_z}{\bar{v}} \left[\frac{\mu(\bar{\lambda})}{m} - \mu_1(\bar{\lambda}) \left(\frac{1 - \bar{\lambda}}{m} + \frac{r^2}{J} \right) \right] \delta \lambda + \frac{r}{J\bar{v}} \delta T_b \quad (6.9)$$

Thus, the transfer function $G_\lambda(s)$ from input δT_b to output $\delta \lambda$ takes the form:

$$G_\lambda(s) = \frac{\frac{r}{J\bar{v}}}{s + \frac{mg}{\bar{v}} \left[\mu_1(\bar{\lambda}) \left((1 - \bar{\lambda}) + \frac{mr^2}{J} \right) - \mu(\bar{\lambda}) \right]} \quad (6.10)$$

As discussed in [27], we can define the **Plant transfer function** $G_\lambda(s)$ in first order form:

$$G_\lambda(s) = \frac{k_i}{s + p_i} \quad (6.11)$$

with a gain:

$$k_i = \frac{r}{J\bar{v}} \quad (6.12)$$

and a single pole of:

$$p_i = \frac{mg}{\bar{v}} \left[\mu_1(\bar{\lambda}) \left((1 - \bar{\lambda}) + \frac{mr^2}{J} \right) - \mu(\bar{\lambda}) \right] \quad (6.13)$$

The vehicle speed v is always positive (forward driving assumption), its variation cannot make the plant unstable but the speed can value will impact on the transfer function gain(k_i).

On the other hand, the change of μ_1 will move the location of pole on s plan, which will have an effect on the stability of plant. More specifically, the effect of μ_1 variation dynamics is significant as it can make the plant unstable.

Considering a typical longitudinal friction/slip curve, as shown in Figure (3.3), we can conclude from the pole equation 6.13 that the open transfer function $G_\lambda(s)$ is:

- **Stable** before slip peak (as $\mu_1 > 0$, therefore $p_i > 0$)
- **Unstable** when the slip goes beyond the peak point (as $\mu_1 < 0$, therefore $p_i < 0$)
- **Pure Integrator** when the linearization point is close to the peak of the curve($\mu_1 \cong 0$):

$$G_\lambda(s) = \frac{k_i}{s} \quad (6.14)$$

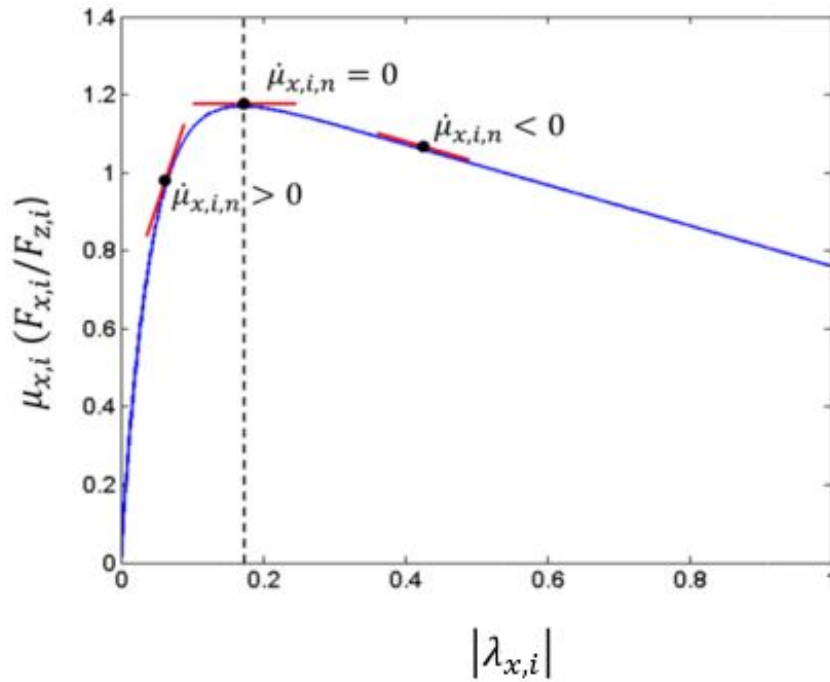


Figure 6.8: Slope of μ at different operating points

6.3 Control approach

The nonlinear behaviour of the system, discussed in the previous Sections, not allows to use a normal PID control for all the different braking condition. The most critical point is around the peak of grip coefficient μ_{max} .

The input-output curve could be divided in two part using as threshold the optimal slip ratio value, which provides the maximum grip coefficient:

$$\lambda_o = \underset{\lambda}{\operatorname{argmax}} \mu(\lambda) \quad (6.15)$$

The input-output curve can be divided in two part:

1. The **normal brake phase**, $[0, \lambda_o]$ which the the system is stable and it is possible to control the braking using the speed error as a input;
2. The **critical brake phase**, in the range $[\lambda_o, 1]$ which is a dangerous zone and the ABS will be activated. In this zone the braking control is focused on the reach a stable value of slip ratio that allow to have the highest brake effort possible. So that, the input used is the error from the optimal slip ratio λ_o , that allows to avoid ABS activation and have the highest deceleration possible;

To control this system is clear that only one linear controller is not feasible, for this reason the idea is to implement an "Hybrid Gain Scheduling" A with two different controller and a proper switch logic to swap between them.

1. **PID - Speed error control:** when the speed error requires a normal braking manoeuvre . The gains value for the Proportional, Integration and Derivation controller must be tuned, in order to follow the speed target rapidly but also enough smooth to avoid loss of comfort in the car. The control input is v_e and the slip ratio is in the stable region;
2. **PID - Slip ratio control:** when the slip ratio in near to the critical value, due to an hard or urgency braking. The Proportional, Integration and Derivation controller gains must be tuned in order to reach as soon as possible the slip ratio target λ_o , in order to return in the stable slip interval. The control input is the slip ratio error $\epsilon_\lambda = \lambda_o - \lambda$ and the slip ratio is in the unstable region;

6.4 Switch Logic

In order to switch between the different controllers a switch logic is developed, which the value of slip ratio is used as inputs of the switch logic system.

A comparator with hysteresis is implemented with the relative thresholds, this addition on the switch logic is useful to avoid oscillation. The thresholds values need to be tuned using the simulation results.

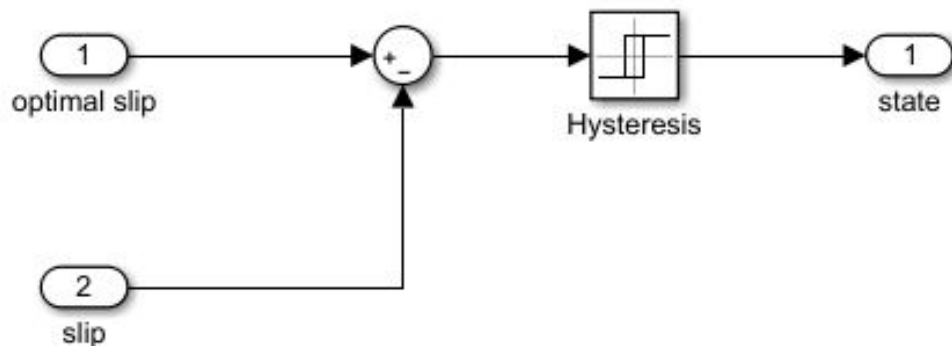


Figure 6.9: Switch logic system with hysteresis

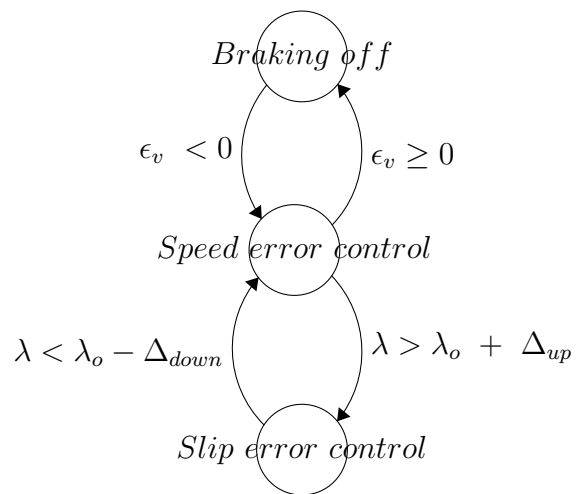
The switch logic approach is:

- If the slip ratio is less than $< \lambda_o - \Delta_{down}$ the PID - Speed error controller is used;
- If the slip ratio is more than $> \lambda_o + \Delta_{up}$ the PID - Slip ratio controller is used;

This behaviour can be draw as a state machine, where the first condition is to have a brake request due to a negative speed error, which means that a braking effort is needed.

The slip ratio is monitored during the braking to understand if it is needed to pass in the slip error control, due to an override of the target slip value.

If it is necessary, the system remains on it until the slip value returns again below the target value.



The performance of this solution is strictly related to the value of the optimal ratio, that needs to be discussed furthermore.

6.5 Optimal slip

The value used to compare and chose which controller should be the optimal slip ratio 6.15, which is difficult to estimate in real application due to the road-tyre conditions variation.

A first approach is to use the method of the Anti-lock Braking System, which is an electronic control system implemented in all the modern cars. It uses electrical-valves to decrease the pressure in the brake hydraulic circuit, in order to remain into the stable area $\lambda \in [0, \lambda_o]$.

In general, a good choice is to use the optimal slip ratio for the dry asphalt. This allows to have the high deceleration during an emergency braking in the most common conditions and to maintain a driveability of the vehicle, because the wheels are not locked-up.

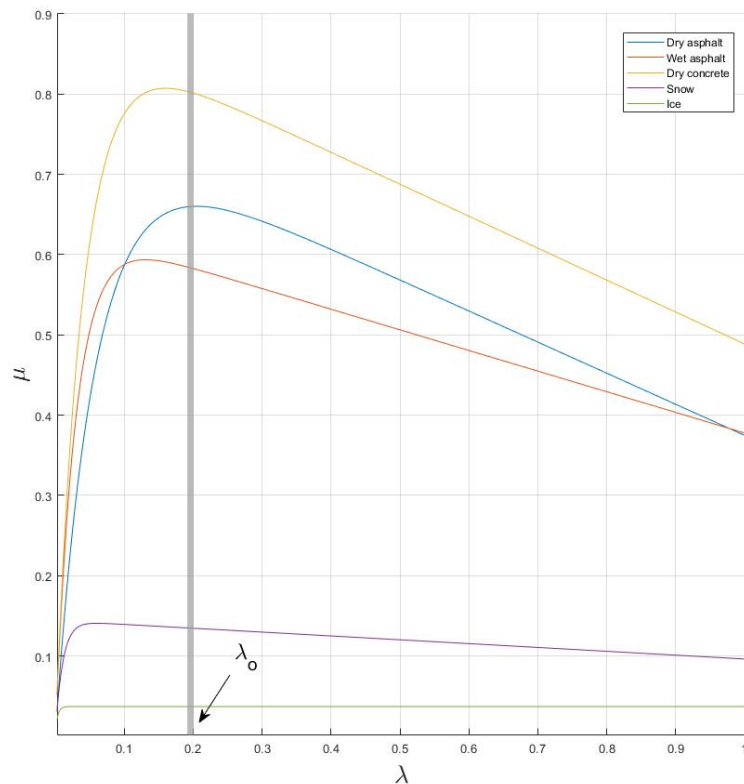


Figure 6.10: A fix λ_o in comparison with different road condition

In the other hand, as shown in Figure (6.10), it is not possible to have the

maximum deceleration and driveability if the asphalt is not dry or in a good condition.

The braking performances could be optimize with an estimation of the optimal slip ratio, in order to have a not-fixed value, but a target slip ratio that adapts to different situations.

This new approach needs to estimate in real time the optimal slip value, that is an open point in the car braking analysis. This is due to the difficult to have a real-time grip coefficient behaviour using only the values collected from the sensors typically installed on the car.

Assumed that the derivative of the grip coefficient is available, it is possible to found an algorithm to save and update the current slip ratio value. It is possible using the characteristic of the grip coefficient curve, for which the slope becomes equal to zero at the peak, the related slip value is the optimal one.

To avoid a collection of wrong optimal slip ratio, during situation of soft braking, it is needed to collect the data only when there is an hard braking for an high value of speed error (e.g. $\epsilon_v > 5m/s$). Therefore the conditions are:

$$\text{IF } \epsilon_v < -5m/s \text{ AND } \dot{\mu} < 0.15 \text{ AND } \dot{\mu} > 0.14 \longrightarrow \lambda_o = \lambda$$

The thresholds values have been set using model simulation on Simulink, in which the performance and robustness of the system has been evaluated for different threshold values.

The disturbances have been added to the grip coefficient on the model simulation, in order to have a more realistic simulation.

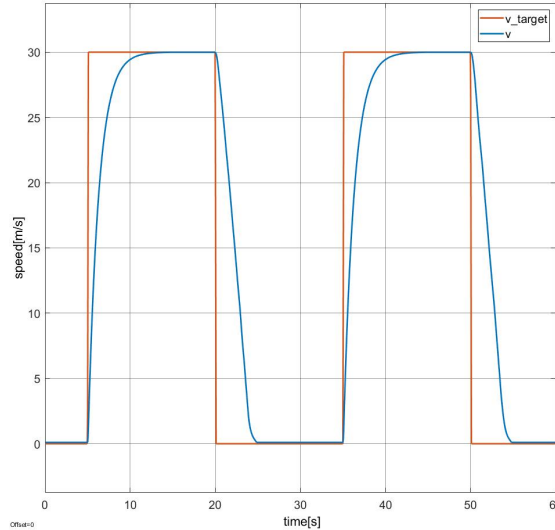


Figure 6.11: Speed error for a sequence of the same braking request

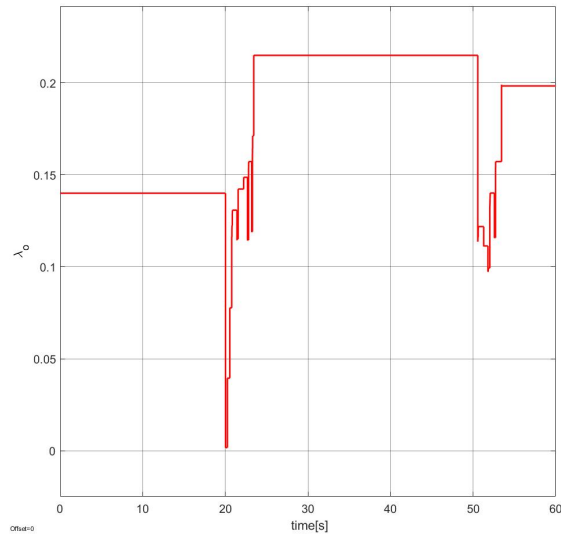


Figure 6.12: Optimal slip ratio value estimated

It is possible to note in Figure (6.12), that for the same braking sequence the optimal slip ratio is corrected using the slip peak detection. In this way the braking system can adapt itself to the road condition.

In literature, there are different methods to find the derivative of the grip coefficient, for example in [26] is used the *Detection of the Friction-curve Peak by Wheel-deceleration Measurements*.

Chapter 7

Simulations results

Matlab and Simulink are used to collect data of the system behaviour and to tune the PIDs gains and threshold values.

The braking system of the Citroën e-Méhari is taken as sample for this thesis, using values measured on the vehicle and values from similar vehicle for measurements when not available, summarized in table 7.1.

	Symbol	Value	Unit
Car mass	M	1405	kg
Quarter-car mass	m	351.25	kg
Wheel radius	r	0.32	m
Wheel Inertia Moment	J	1.17	kg/m^2
Gravity acceleration	g	9.81	m/s^2
Disc-pads coefficient of kinetic friction	μ_{disc}	0.38	
Center of the wheel - disc braking application point	r_m	0.185	m
Number of brake pads in disc brake assembly	N	2	
Wheel cylinder piston's area	A_{cw}	0.0015	m^2
Pedal ratio	τ_p	3.4	
Servomotor time lag	τ_{servo}	0.2	s

Table 7.1: Vehicle data used in the model simulation

During the simulations, it was possible to check the system response and tuning

the controllers and switch logic parameters. In this regard the characteristics used to analyze the system performance are:

- Speed error: the system should be able to follow the target speed;
- Braking distance: mainly in the urgent braking, it should be as short as possible;
- Stopping time: mainly in the urgent braking, it should be in the lowest time possible;
- Slip ratio: it should not be too high and principally should be always far to the unitary value and in any case;
- Deceleration: the deceleration should be not too high during the normal driving to not lead the user comfort, but it should be the highest possible in case of urgent braking;
- Controller output: this is the pedal travel that should be changed during the system working in a feasible way. A quick and frequent request of the pedal position movement could be not feasible in real application;

The selected values for controllers and switch logic parameters are in 7.2.

System	Parameter	Value
Switch logic	Δ_{up}	0
	Δ_{down}	-0.01
PID - Speed error control	Proportional	-13
	Integral	-0.08
	Derivative	-2
	Filter	100
PID - Slip error control	Proportional	100
	Integral	1
	Derivative	10
	Filter	1000

Table 7.2: Controllers and switch logic parameters

7.1 Hard braking test

Starting from a initial speed $v_0 = 30 \text{ m/s}^2 \approx 100 \text{ km/h}$ an hard and urgent braking is simulated. In this case the speed input is a step 7.1 that after 5 s go from 30 m/s to 0 m/s . This simulation allows to activate the Slip controller due to the high deceleration required. In this way it is possible to test and set the parameters in the second PID, switch logic, hysteresis and optimal slip estimator.

In this situation the goal is to have the higher deceleration possible, in order to stop the vehicle in the shortest time and distance, for example in case of an unexpected crossing of a pedestrian.

Different road conditions are simulated and in order to test the system robustness will be also add a random source is adding to the grip coefficient, in order simulate the continuous changing of this value due to the real world complexity, for example it is very common to have an asphalt where the water quantity changes during the driving.

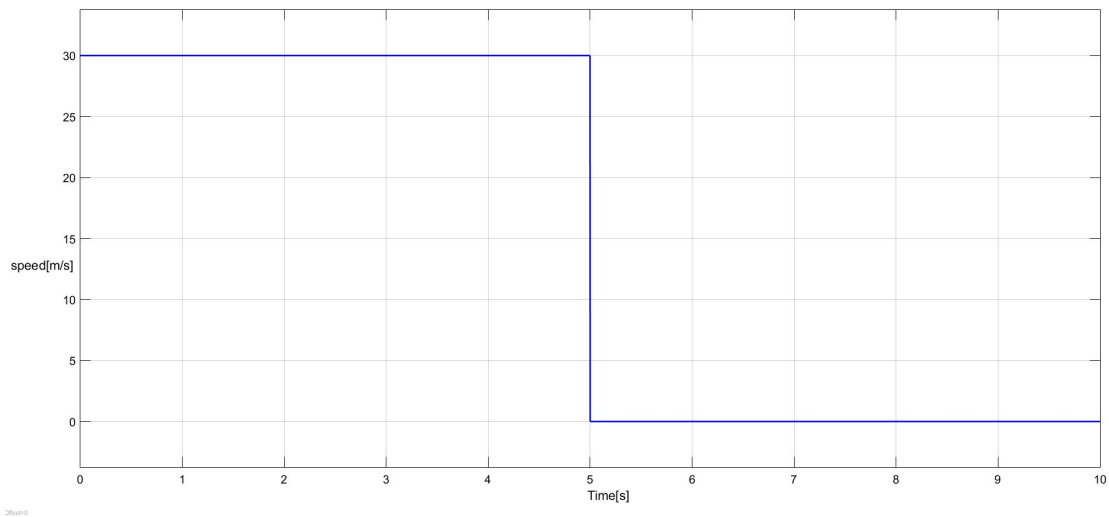


Figure 7.1: Speed target step for hard braking test

7.1.1 Without slip PID controller

The first simulation is only with a speed error controller, without the controller used to control the slip. In this condition the system becomes unstable during the braking, the wheels skids and there is a loss of drivability and deceleration value as showed in 7.2,7.3 and 7.4.

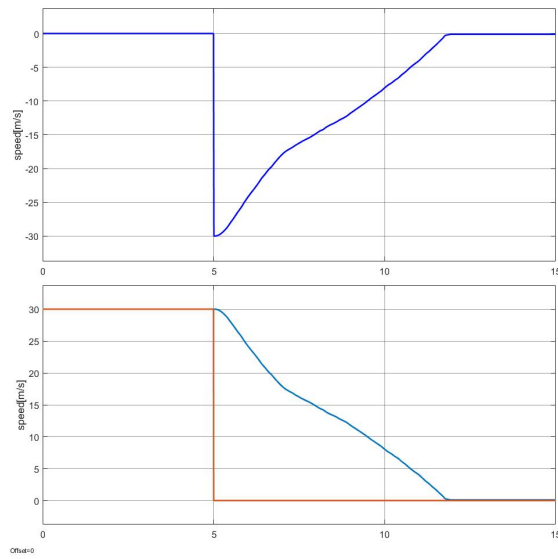


Figure 7.2: Speed error ϵ_v and v_{target} $v_{vehicle}$ simulation results - Without slip PID controller

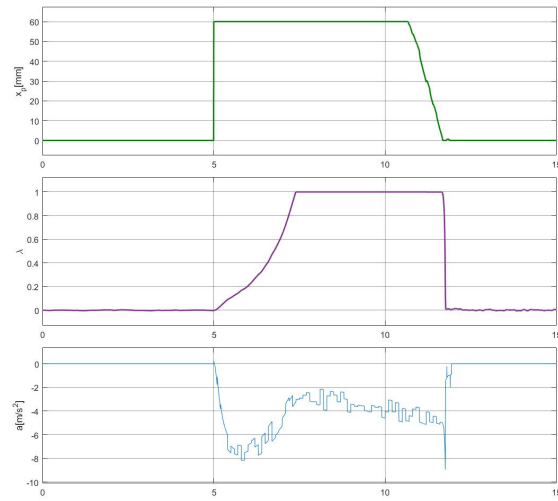


Figure 7.3: Controller input[mm], slip ratio and vehicle acceleration simulation results - Without slip PID controller

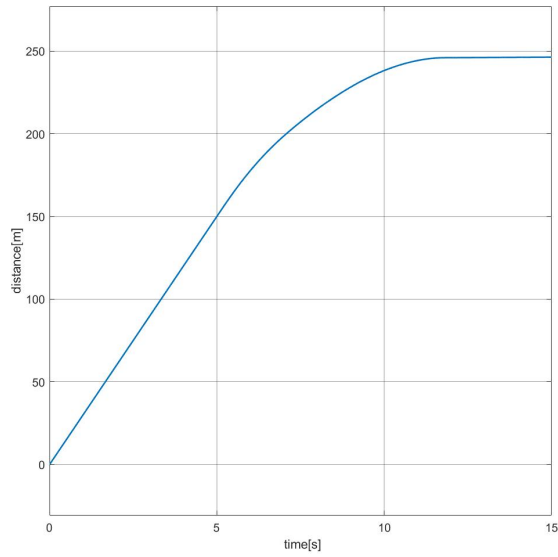


Figure 7.4: Vehicle distance - Without slip PID controller

The numerical results in 7.3 show that the stopping distance is long, the time needed is high, the maximum deceleration is not so high and the slip ratio tends rapidly to 1.

Braking distance	96.31	m
Stopping time	6.94	s
λ_{max}	1	
a_{min}	-8.95	m/s^2

Table 7.3: Without slip control numerical results

7.1.2 Using slip PID controller

In system is added the PID controller for the slip ratio and the switch logic, which are able to maintain the car braking in the stable operating points. This allows to increase the value of deceleration achieved, have enough drive-ability, that bring to a reduction of the time and distance required to stop the vehicle, as showed in 7.5, 7.6 and 7.7.

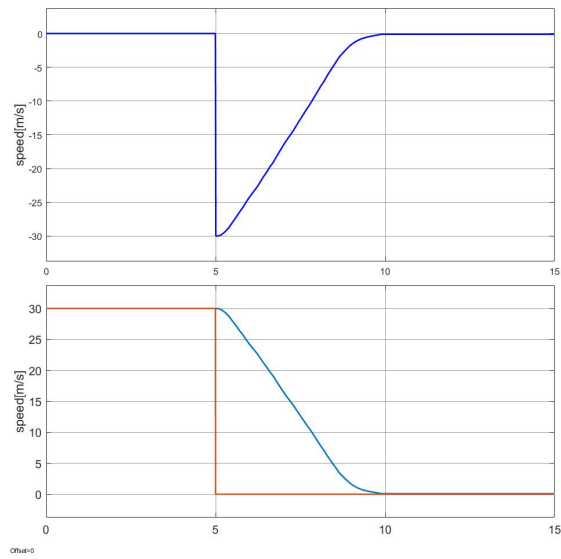


Figure 7.5: Speed error ϵ_v and v_{target} $v_{vehicle}$ simulation results - Using slip PID controller

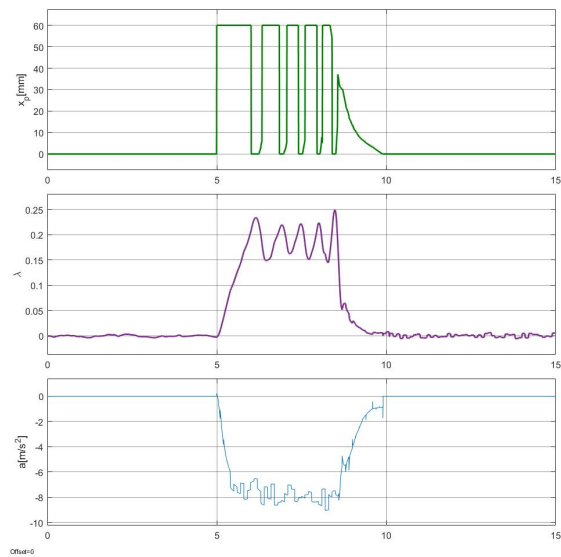


Figure 7.6: Controller input[mm], slip ratio and vehicle acceleration simulation results - Using slip PID controller

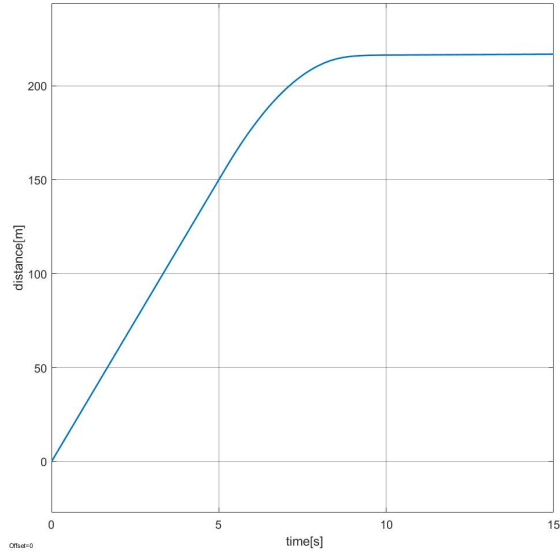


Figure 7.7: Vehicle distance - Using slip PID controller

In this case the optimal slip ratio used in the switch logic is fixed to 0.18. It can be considered a good trade off, which allows to have a good performance without loss of stability for almost all the driving situation.

The numerical results in 7.4 show the improvements reached with the adding of a designed slip control, in comparison with the previous case with only the speed controller. The braking maneuver now is more safe in all point of view.

Braking distance	66.31	<i>m</i>
Stopping time	4.91	<i>s</i>
λ_{max}	0.25	
a_{min}	-9.08	<i>m/s²</i>

Table 7.4: With slip control numerical results

7.1.3 Different road conditions: Wet asphalt

The previous simulation were with the Burckhardt coefficients for the dry asphalt, but it is possible to demonstrate that also for a different road status the control system responds in a proper way, as showed in 7.8,7.9 and 7.10 for wet asphalt.

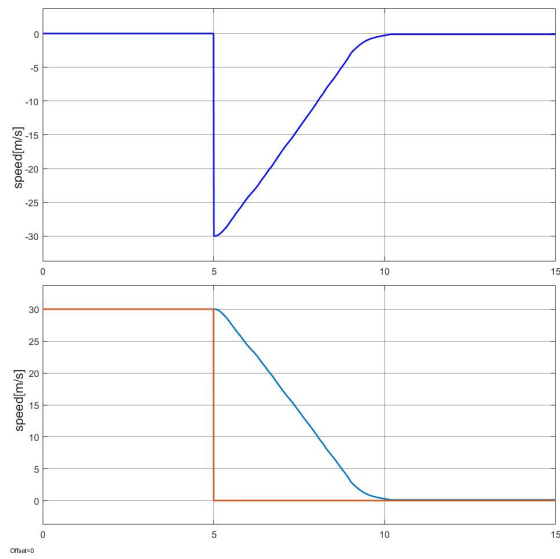


Figure 7.8: Speed error ϵ_v and v_{target} $v_{vehicle}$ simulation results - Wet asphalt and fixed optimal slip

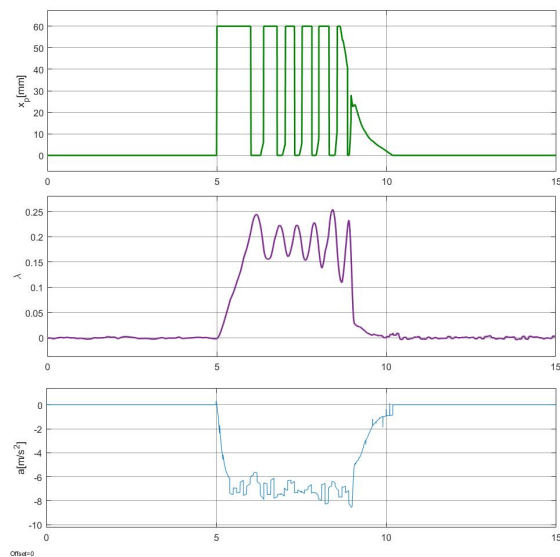


Figure 7.9: Controller input[mm], slip ratio and vehicle acceleration simulation results - Wet asphalt and fixed optimal slip

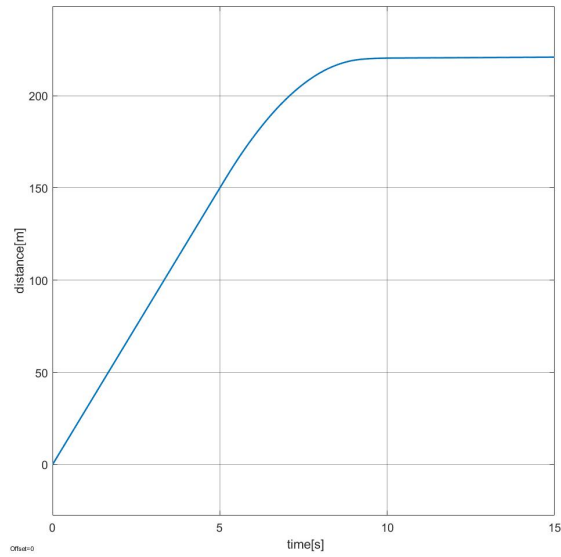


Figure 7.10: Vehicle distance - Wet asphalt and fixed optimal slip

The previous simulation is with the optimal slip ratio fixed to 0.18, that is a good trade-off but it is not the best value of optimal slip. Using the optimal slip calculation explained in 6.5 it is possible to found a value that improve the performance for different road condition, as showed in 7.11 the value used is $\lambda_o \approx 0.16$.

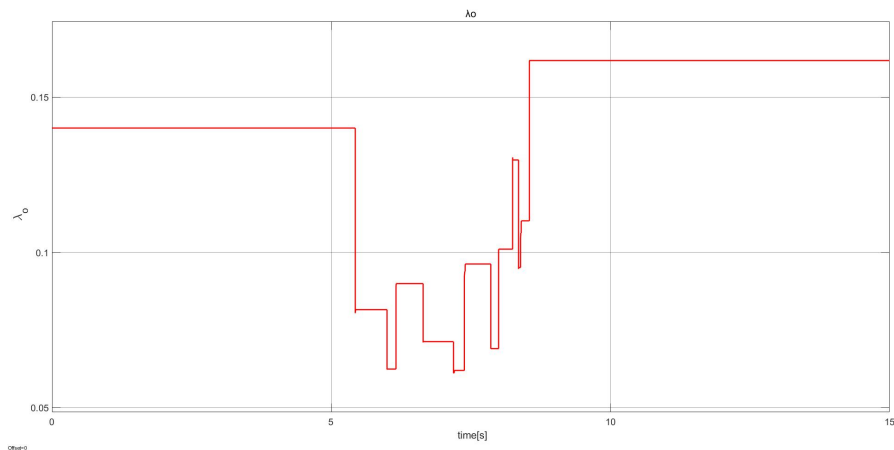


Figure 7.11: Optimal slip estimation during the braking - Wet asphalt

In this case the results are showed in 7.8,7.9 and 7.10 for wet asphalt.

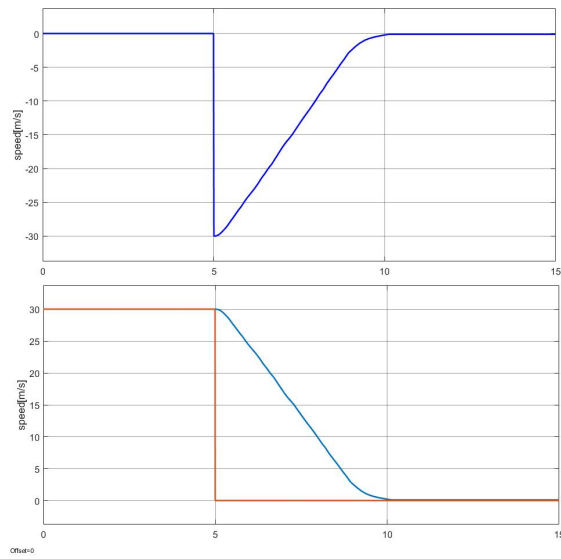


Figure 7.12: Speed error ϵ_v and v_{target} $v_{vehicle}$ simulation results - Wet asphalt and estimated optimal slip

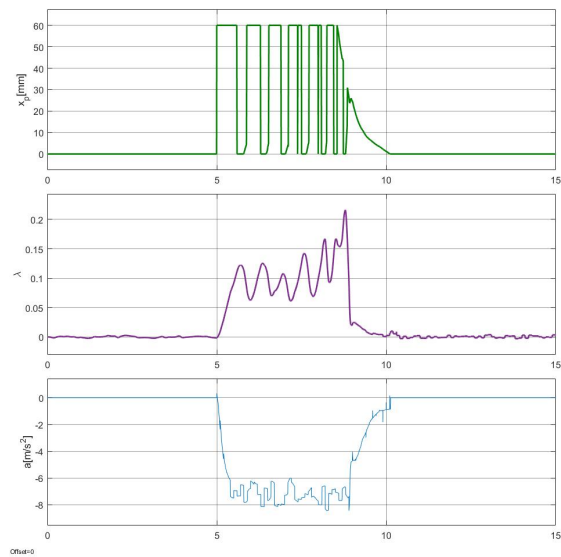


Figure 7.13: Controller input[mm], slip ratio and vehicle acceleration simulation results - Wet asphalt and estimated optimal slip

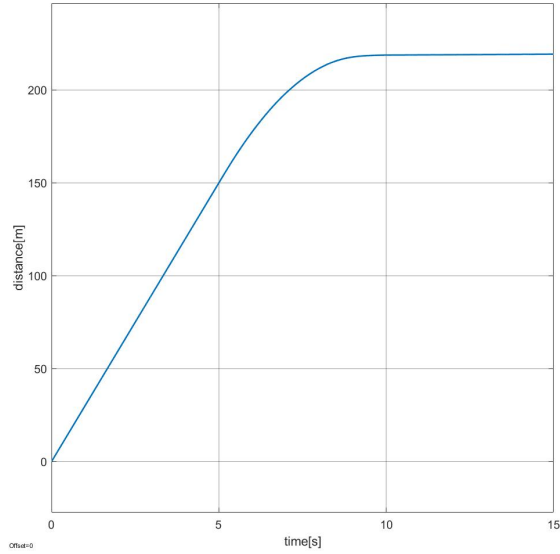


Figure 7.14: Vehicle distance - Wet asphalt and estimated optimal slip

The numerical results in 7.5 put in comparison the two different approach for the definition of the optimal slip ratio value. There is a little improvement with the dynamic optimal slip ratio, mainly for the slip ratio that is more near to the peak grip(w.r.t. figure3.5), that means to have more system stability.

	fixed λ_o	estimated λ_o	
Braking distance	70.41	69.29	m
Stopping time	5.19	5.13	s
λ_{max}	0.25	0.21	
a_{min}	-8.56	-8.44	m/s^2

Table 7.5: Different slip control approach numerical results - Wet asphalt

The stopping time increases of $\approx 0.3s$ in comparison of the dry asphalt test, due to a degradation of the road-tyre condition.

7.1.4 Different road conditions: Snow

The snow condition is one of the worst case for the braking maneuver, but in 7.15,7.16 and 7.17 is showed that the braking is stable, with a obviously huge increasing of the stopping time.

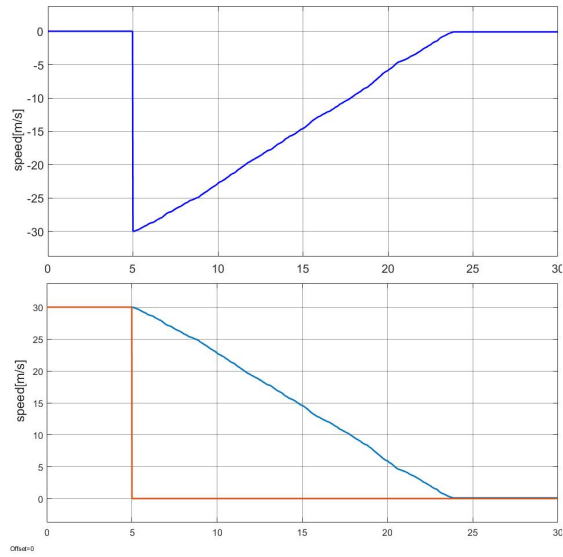


Figure 7.15: Speed error ϵ_v and v_{target} $v_{vehicle}$ simulation results - Snow and fixed optimal slip

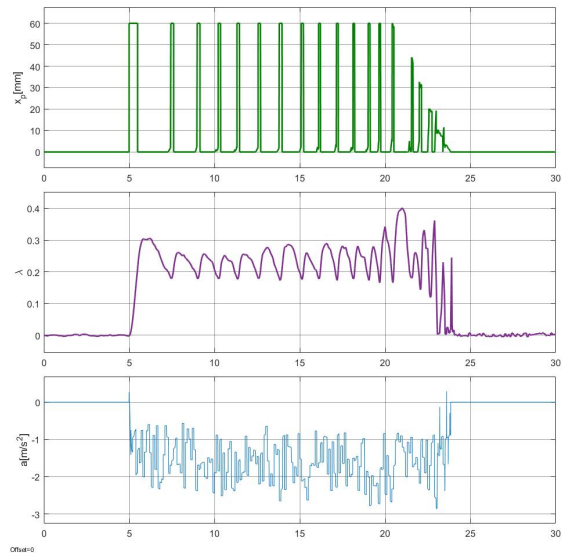


Figure 7.16: Controller input[mm], slip ratio and vehicle acceleration simulation results - Snow and fixed optimal slip

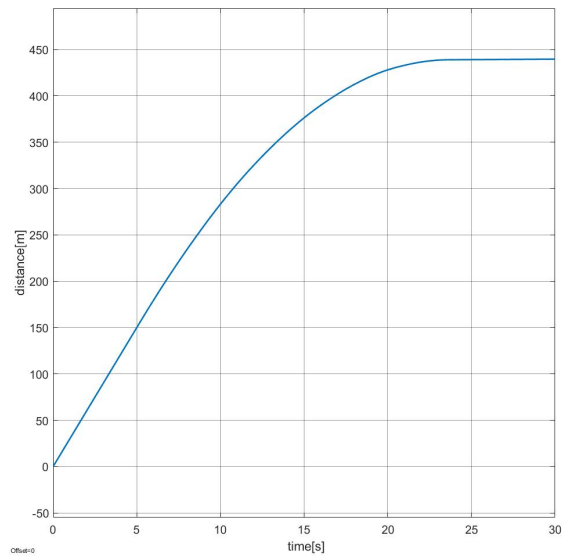


Figure 7.17: Vehicle distance - Snow and fixed optimal slip

In this critical scenario is more clear that the maximum value of grip coefficient and so of deceleration have a dynamic dependence of the slip target used as input, for this reason the dynamic choice of the optimal slip ratio improves the braking performance, as showed in 7.18,7.19 and 7.20.

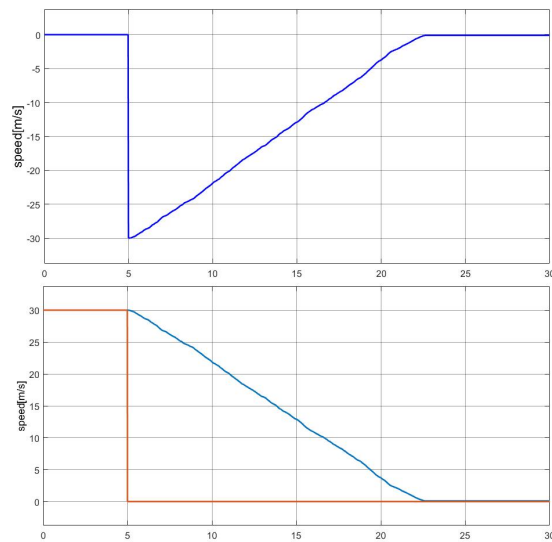


Figure 7.18: Speed error ϵ_v and v_{target} $v_{vehicle}$ simulation results - Snow and estimated optimal slip

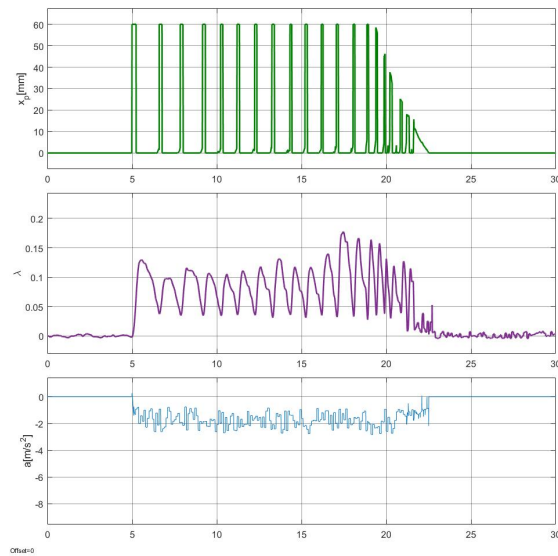


Figure 7.19: Controller input[mm], slip ratio and vehicle acceleration simulation results - Snow and estimated optimal slip

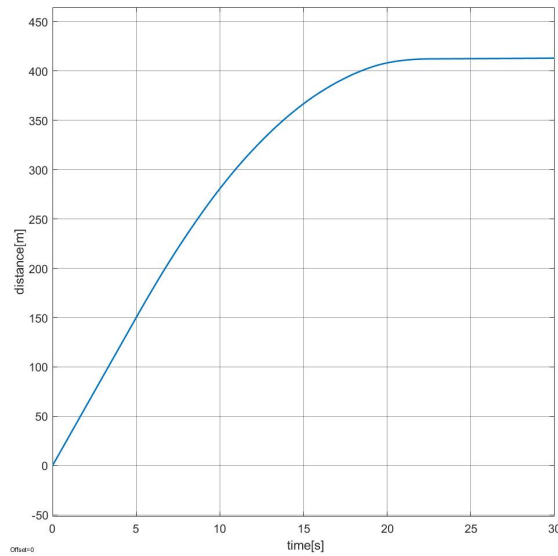


Figure 7.20: Vehicle distance - Snow and estimated optimal slip

The numerical results 7.6 for this test time demonstrate the difference of the two approach more evidently. This is due to the estimated optimal slip ratio that is more similar to real one.

	fixed λ_o	estimated λ_o	
Braking distance	289.7	263.1	<i>m</i>
Stopping time	18.84	17.52	<i>s</i>
λ_{max}	0.40	0.18	
a_{min}	-2.86	-2.834	<i>m/s²</i>

Table 7.6: Different slip control approach numerical results - Snow

7.2 Drive Cycle test

The homologation drive cycle is used to evaluate the system, where the output is the speed target in $[m/s]$.

The EPA New York City Cycle (NYCC) has been simulated, it lends itself to evaluate the control system developed in a real world test.

In order to perform this test in a proper way, I added in the Simulink model a proportional controller, in order to accelerate when is needed and follow the speed target also when the speed error is negative.

Another switch logic is added to avoid oscillation during the switching between the acceleration and deceleration request.

The simulation results are showed in 7.21 and 7.22. The control system designed is able to make a common city drive cycle using only the speed error controller, due to the fact it is not needed to have an urgency braking.

The maximum slip ratio is maintained low ≈ 0.025 and the maximum deceleration reached is around the values of $3m/s^2$ recommended by AASHTO, therefore it does not affect the driver comfort.

The maximum speed error is less than $-1m/s$ that is acceptable and it should be not appreciable from the driver.

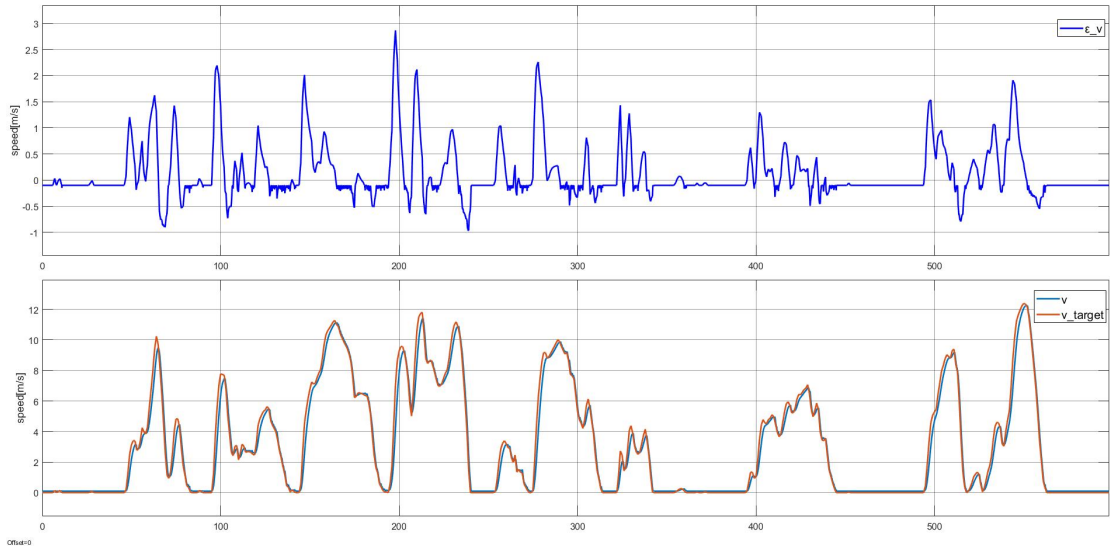


Figure 7.21: Speed error ϵ_v and v_{target} $v_{vehicle}$ simulation results

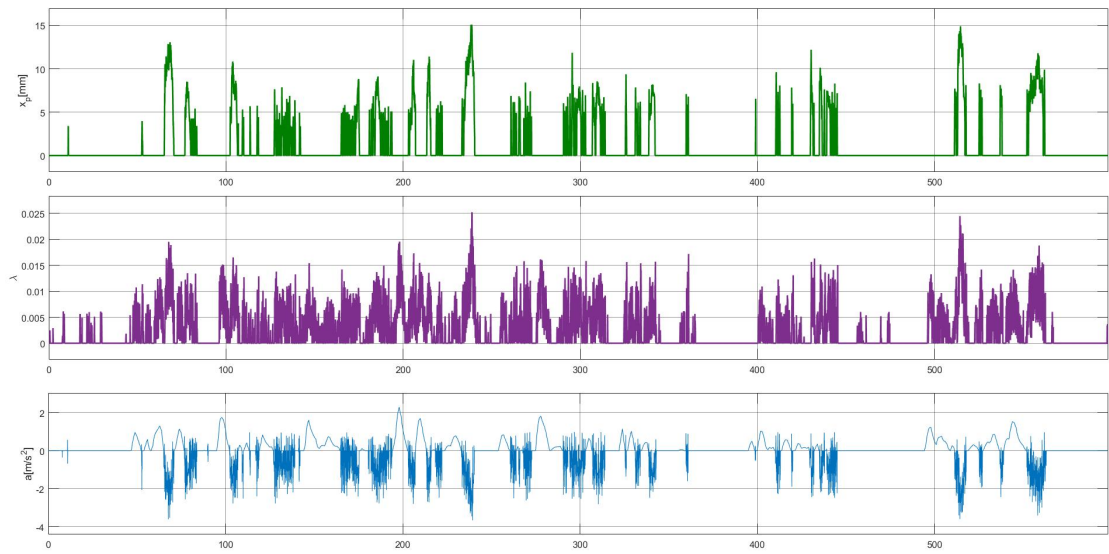


Figure 7.22: Controller input[mm], slip ratio and vehicle acceleration simulation results

Chapter 8

Conclusions

In this dissertation, I designed a different way to implement an autonomous braking system concerning the brake-by-wire system. The aim is to design a system implementable on a real vehicle.

Using the literature it has been possible to develop a physical model, that takes into account the braking system installed on the car in terms of mechanical and hydraulic components.

The system is complex due to the non-linear behaviour of the vacuum booster and the tyre-road friction coefficient. The last one needs to be treated using the Burckhardt model, computed by theoretical deformation and simulation.

An electromechanical actuator is designed to be the interface between the autonomous driving unit and the brake pedal. This feature allows the system to be integrated into a car without radical changes, as opposed to the brake-by-wire solution.

The whole system has been simulated using Simulink and after the first tuning of the controllers and the switch logic parameters, it was possible to evaluate the performance and compare the different approaches.

In case of hard braking, the PID speed error control is not able to maintain stability of the car and the ABS is always activated.

The hybrid gain scheduling with two PID controllers and switch logic support is able to follow the speed target and is safer and more stable in comparison to the previous control solution considered in all braking conditions.

A slip target is used for the PID slip error control and for the switch logic transition. It can be chosen in two different ways.

The first approach uses a fixed target slip using a good trade-off of good deceleration and driveability in any condition. This solution is similar to the normal ABS system used on the common cars.

The second approach uses an estimated optimal slip ratio as target and allows to have theoretically the best performance during the braking. A good estimation is difficult and is strongly related to the typologies of the sensors and data available during the driving.

The system performance has been found good in terms of user safety and comfort. It performs well for all the braking typologies tested.

8.1 Future works

Based on the analysis and project developed in this thesis, further studies can be performed and different applications may be worth examining:

- The car cornering can be implemented on the simulation, in order to consider driving scenarios closer to the real world;
- The dynamic changing of the vertical load can be implemented on the single-wheel model;
- Implementation of the electromechanical actuator designed on the real car. In order to validate the robustness and performance in a real-world application, the parameters tuning and subsequent tests should be properly performed;
- Implementation and comparison of different optimal slip ratio estimator and relative implementation, to evaluate the feasibility of the different solutions in a real system;
- Comparison with the brake-by-wire solution;

Appendix A

Gain scheduling

The gain scheduling is used on plant linearized around equilibrium point, in order to use a linear feedback controller also in a non-linear model.

As explained in [28] the first step is to define the points of operation, analyse it and choose a proper linear controller able to work with the plant in an predetermined region around the point chosen.

Using an interpolation function with a proper switch logic possible to obtain a unique controller able to operate in all the regions.

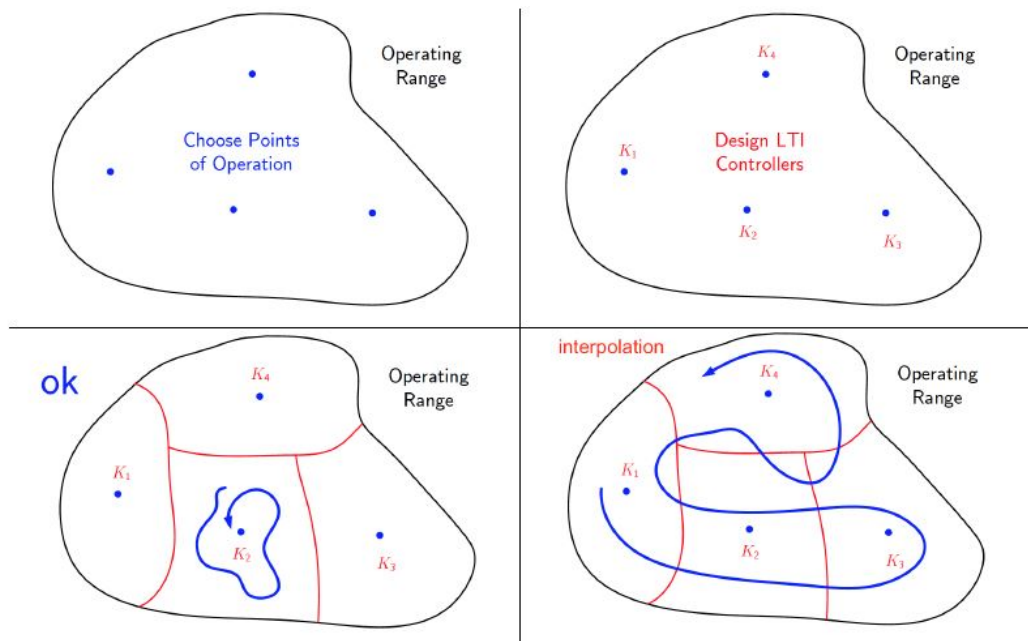


Figure A.1: Gain scheduling operating range

Consider a generic system:

$$\begin{aligned}\dot{x} &= f(x, u, w) \\ \dot{y} &= h(x)\end{aligned}\tag{A.1}$$

In which f and h are differentiable functions on suitable domains D_f, D_h . The state is $x \in \mathbb{R}^{n_x}$, the command input $u \in \mathbb{R}^{n_u}$ and $y \in \mathbb{R}^{n_y}$ is the output. In order to individuate the operating point is used a measured signal called scheduling variable:

$$\bar{w}_1, \dots, \bar{w}_N \subset D_w \subseteq \mathbb{R}^{n_w}\tag{A.2}$$

For each of $\bar{w}_i \in D_w$, a pair of (\bar{x}_i, \bar{u}_i) has to be found, such that $(\bar{x}_i, \bar{u}_i, \bar{w}_i)$ is an equilibrium point of (A.1). In particular:

$$f(\bar{x}_i, \bar{u}_i, \bar{w}_i) = 0, \quad i = 1, \dots, N\tag{A.3}$$

As based on this the nonlinear system (A.1) can be linearized around each equilibrium point $(\bar{x}_i, \bar{u}_i, \bar{w}_i)$ with a definition of these variables:

$$\begin{aligned}\tilde{x}_i &\doteq x - \bar{x}_i \\ \tilde{u}_i &\doteq u - \bar{u}_i \\ \tilde{w}_i &\doteq w - \bar{w}_i \\ \tilde{y}_i &\doteq y - h(\bar{x}_i)\end{aligned}\tag{A.4}$$

The state equations of the linearized system are:

$$\begin{aligned}\dot{\tilde{x}}_i &= A(\bar{w}_i)\tilde{x}_i + B(\bar{w}_i)\tilde{u}_i + E(\bar{w}_i)\tilde{w}_i^e \\ \tilde{y}_i &= C(\bar{w}_i)\tilde{x}_i\end{aligned}\tag{A.5}$$

The matrix of the state space are:

$$\begin{aligned}A(\bar{w}_1) &\doteq \left. \frac{\delta f}{\delta x} \right|_{(\bar{x}_i, \bar{u}_i, \bar{w}_i)} & B(\bar{w}_1) &\doteq \left. \frac{\delta f}{\delta u} \right|_{(\bar{x}_i, \bar{u}_i, \bar{w}_i)} \\ E(\bar{w}_1) &\doteq \left. \frac{\delta f}{\delta w_e} \right|_{(\bar{x}_i, \bar{u}_i, \bar{w}_i)} & C(\bar{w}_1) &\doteq \left. \frac{\delta h}{\delta x} \right|_{(\bar{x}_i, \bar{u}_i, \bar{w}_i)}\end{aligned}\tag{A.6}$$

The superscript "e" is for the component of w that are external inputs. Now, with this structure is possible to design LTI controllers for each LTI system A.5, using any desired technique (i.e. in this dissertation a PID controllers are used). The i -th controller is defined by the general control law:

$$\begin{aligned}\tilde{u}_i &= K_i(\tilde{e}_i) = K_i(e) \\ \tilde{e}_i &\doteq \tilde{r}_i - \tilde{y}_i = r - h(\bar{x}_i) - y + h(\bar{x}_i) = r - y = e\end{aligned}\tag{A.7}$$

Where e is the tracking error and r is the reference signal.

The controllers K_i are characterized by the same structure but different values of their parameters:

$$K_i(e) = K(p_i; e)$$

Where $p_i \in \mathbb{R}^{n_p}$ is the vector of all controller parameters and this vector depends on the operating point \bar{w}_i .

Each controller $K(p_i; e)$ is local, in the sense that it works correctly in some neighborhood of the i -th operating point.

The **global controller** is defined by the control law:

$$u = \mathcal{I}_u(w) + K(\mathcal{I}_p(w); e) \quad (\text{A.8})$$

The suitable interpolation functions is $\mathcal{I}_u(w)$, such that, for $i = 1, \dots, N$, there are:

$$\begin{aligned} \mathcal{I}_p(\bar{w}_i) &= p_i \\ \mathcal{I}_u(\bar{w}_i) &= \bar{u}_i \end{aligned}$$

A simple look-up table or a designed switch logic are often used as interpolation function.

PID It is the linear controller used in this thesis, it has simple structure, with only 3 parameters (Proportional, Derivative and Integrator).

In Laplace domain, with s as variable, it is possible to define the PID controller in the form:

$$K(s) = c_P + \frac{C_I}{s} + C_D s \quad (\text{A.9})$$

If also the filter parameter c_N is implemented (to allow the derivative term implementation), the PID structure become:

$$K(s) = c_P + \frac{C_I}{s} + c_D \frac{c_N}{1 + c_N \frac{1}{s}} \quad (\text{A.10})$$

The parameters are function of the scheduling variable:

$$\begin{aligned} c_P &= c_P(w) \\ c_I &= c_I(w) \\ c_D &= c_D(w) \\ c_N &= c_N(w) \end{aligned} \quad (\text{A.11})$$

These values are obtained with trial and error tuning with a whole system test and simulation.

Bibliography

- [1] N. D’alfio, A. Morgando, and A. Sorniotti. «Electro-hydraulic brake systems: Design and test through hardware-in-the-loop simulation». In: *Vehicle System Dynamics* 44 (Jan. 2006), pp. 378–392. DOI: 10.1080/00423110600872291 (cit. on p. 1).
- [2] Venkata Mamilla and M. Mallikarjun. «Control of ElectroMechanical Brake with Electronic Control Unit». In: (Dec. 2021) (cit. on p. 1).
- [3] Xiaoxiang Gong, Weiguo Ge, Juan Yan, Yiwei Zhang, and Xiangyu Gongye. «Review on the Development, Control Method and Application Prospect of Brake-by-Wire Actuator». In: *Actuators* 9 (Mar. 2020), p. 15. DOI: 10.3390/act9010015 (cit. on p. 1).
- [4] Sahil Jitesh. «ANTILOCK BRAKING SYSTEM (ABS)». In: *International Journal of Mechanical Engineering and Robotics Research* 3 (Oct. 2014), p. 253 (cit. on p. 1).
- [5] Reza Hoseinnezhad and Alireza Bab-Hadiashar. «Efficient Antilock Braking by Direct Maximization of Tire–Road Frictions». In: *Industrial Electronics, IEEE Transactions on* 58 (Sept. 2011), pp. 3593–3600. DOI: 10.1109/TIE.2010.2081951 (cit. on p. 1).
- [6] *Uniform provisions concerning the approval of vehicles of categories M, N and O with regard to braking*. Regulation No 13 of the Economic Commission for Europe of the United Nations (UN/ECE). 2016/194 (cit. on p. 4).
- [7] *Consolidated Resolution on the Construction of Vehicles (R.E.3), Revision 6*. Economic Commission for Europe. 2014 (cit. on p. 4).
- [8] Lorenzo Morello Giancarlo Genta, ed. *The Automotive Chassis*. Springer, 2009 (cit. on p. 5).
- [9] Massimo Violante. *Slides of the course*. Technologies for Autonomous Vehicles. (2019-2020) (cit. on p. 7).
- [10] Konrad Reif, ed. *Brakes, Brake Control and Driver Assistance Systems*. Springer, 2014 (cit. on p. 8).

- [11] Bill K. H. Breuer B. J., ed. *Brake Technology Handbook*. SAE, 2008 (cit. on p. 10).
- [12] *A Policy on Geometric Design of Highways and Streets*. AASHTO: American Association of State Highway and Transportation Officials. 2001 (cit. on p. 11).
- [13] Massimo Canale. *Slides of the course*. Technologies for Autonomous Vehicles. (2019-2020) (cit. on p. 12).
- [14] Carlos Flores, Pierre Merdrignac, Raoul de Charette, Francisco Navas, Vicente Milanés, and Fawzi Nashashibi. «A Cooperative Car-Following/Emergency Braking System With Prediction-Based Pedestrian Avoidance Capabilities». In: *IEEE Transactions on Intelligent Transportation Systems* 20.5 (2019), pp. 1837–1846. DOI: 10.1109/TITS.2018.2841644 (cit. on p. 13).
- [15] Société de Technologie Michelin. «The tyre, Grip». In: *Michelin* (2001) (cit. on pp. 14, 18).
- [16] Manfred Burckhardt, ed. *Fahrwerktechnik, Radschlupf-Regelsysteme*. Vogel, 1993 (cit. on p. 16).
- [17] Hongjun Zhu, Liang Li, Maojing Jin, Hongzhi Li, and Jian Song. «Real-time yaw rate prediction based on a non-linear model and feedback compensation for vehicle dynamics control». In: *Proceedings of the Institution of Mechanical Engineers, Part D: Journal of Automobile Engineering* 227 (Oct. 2013), pp. 1431–1445. DOI: 10.1177/0954407013482070 (cit. on p. 19).
- [18] *What is 'Circle of Friction'?* <https://www.researchgate.net/post/What-is-Circle-of-Friction>. Accessed: 2021-11-27 (cit. on p. 20).
- [19] Jian Zhao, Zhiqiang Hu, Bing Zhu, and Jiapeng Gong. «Integrated model control of brake-wheel system using bond graph method». In: *Advances in Mechanical Engineering* 10 (July 2018), p. 168781401878285. DOI: 10.1177/1687814018782857 (cit. on p. 22).
- [20] *Disc Brake*. <https://it.mathworks.com/help/phymod/sdl/ref/discbrake.html>. Accessed: 2021-11-27 (cit. on p. 24).
- [21] A.W. Orłowicz, M. Mróz, G. Wnuk, O. Markowska, W. Homik, and B. Kolbusz. «Coefficient of Friction of a Brake Disc-Brake Pad Friction Couple». In: *Archives of Foundry Engineering* 16 (Apr. 2016). DOI: 10.1515/afe-2016-0109 (cit. on p. 26).
- [22] *Disc Brakes*. https://www.akebono-brake.com/english/product_technology/product/automotive/disc/. Accessed: 2021-11-27 (cit. on p. 27).
- [23] *How Does a Tandem Master Cylinder Work?* <http://www.britishv8.org/Articles/Tandem-Master-Cylinders.htm>. Accessed: 2021-11-27 (cit. on p. 28).

- [24] *Clutch- and brake-pedal forces*. <https://www.kfz-tech.de/Engl/Formelsammlung/PedalkraefteKupplung.htm>. Accessed: 2021-11-27 (cit. on p. 31).
- [25] Bharat Joshi, Rakesh Shrestha, and Ramesh Chaudhary. «Modeling, Simulation and Implementation of Brushed DC Motor Speed Control Using Optical Incremental Encoder Feedback». In: Oct. 2014 (cit. on p. 37).
- [26] Sergio M. Savaresi and Mara Tanelli, eds. *Active Braking Control Systems Design for Vehicle*. Springer, 2010 (cit. on pp. 42, 51).
- [27] Amir Masoud Soltani and Francis Assadian. «New Slip Control System Considering Actuator Dynamics». In: *SAE International Journal of Passenger Cars - Mechanical Systems* 8 (May 2015). DOI: 10.4271/2015-01-0656 (cit. on p. 44).
- [28] Carlo Novara. *Slides of the course*. Nonlinear control and aerospace applications. (2019-2020) (cit. on p. 71).